Double Deprotonation of Ruthenium(II) Cations Containing 1,2-Dimethyl-Substituted η^6-Arenes. Protonation of the Resulting Exo-Coordinated (*o*-Xylylene)ruthenium(0) Complexes and X-ray Crystal Structures of the Agostic (η^3-Pentamethylbenzyl)ruthenium(II) Complexes $[Ru\{\eta^3\text{-}(HCH_2)(CH_2)C_6Me_4\}\{(Z)\text{-}Ph_2PCH{=}CHPPh_2\}(PMe_2Ph)]PF_6$ and $[Ru\{\eta^3\text{-}(HCH_2)(CH_2)C_6Me_4\}(PMe_2Ph)_3]PF_6$

Martin A. Bennett,* Lai Yoong Goh,[1] Ian J. McMahon, Thomas R. B. Mitchell,[2] Glen B. Robertson, Terence W. Turney, and Wasantha A. Wickramasinghe

Research School of Chemistry, Australian National University, GPO Box 4, Canberra, ACT 2601, Australia

Received January 9, 1992

Treatment of the various ruthenium(II) salts $[Ru(ONO_2)(\eta^6\text{-}1,2\text{-dimethylarene})L_2]NO_3$ and $[Ru(O_2CCF_3)(\eta^6\text{-}1,2\text{-dimethylarene})L_2]PF_6$ with KO-*t*-Bu or $(Me_3Si)_2NNa$ in the presence of a ligand L′ gives *o*-xylylene (*o*-quinodimethane) complexes of zerovalent ruthenium, i.e. $Ru\{\eta^4\text{-}(CH_2)_2C_6Me_4\}L_2L'$ (L = L′ = PMe_2Ph, $P(CD_3)_2Ph$, $PMePh_2$, $P(OMe)_3$, $P(OCH_2)_3CMe$; L_2 = $Ph_2PCH_2CH_2PPh_2$, L′ = PMe_2Ph; L_2 = (*Z*)-$Ph_2PCH{=}CHPPh_2$, L′ = PMe_2Ph, $P(CD_3)_2Ph$), $Ru\{\eta^4\text{-}(CH_2)_2C_6H_2Me_2\}L_2L'$ (L = L′ = PMe_2Ph, $PMePh_2$), and $Ru\{\eta^4\text{-}(CH_2)_2C_6H_4\}(PMe_2Ph)_3$, in good to moderate yields. In all cases the *o*-xylylene group is coordinated through its exo pair of double bonds. The reactions are proposed to proceed via the undetected intermediates Ru(*o*-xylylene)L_2 (L = monodentate P-donor ligand, L_2 = bidentate P-donor ligand) in which the ruthenium atom can migrate from the endo to the exo pair of double bonds before ligand L′ attacks. On treatment with HPF_6, $Ru\{\eta^4\text{-}(CH_2)_2C_6Me_4\}L_2L'$ and $Ru\{\eta^4\text{-}(CH_2)_2C_6H_4\}(PMe_2Ph)_3$ give (η^3-benzyl)ruthenium(II) salts $[Ru\{\eta^3\text{-}(HCH_2)(CH_2)C_6Me_4\}L_2L']PF_6$ (L = $Ph_2PCH_2CH_2PPh_2$, L′ = PMe_2Ph (**1**); L = (*Z*)-$Ph_2PCH{=}CHPPh_2$, L′ = PMe_2Ph (**2**), $P(CD_3)_2Ph$ (**2a**); L = L′ = PMe_2Ph (**3**), $P(CD_3)_2Ph$ (**3a**)) and $[Ru\{\eta^3\text{-}(HCH_2)(CH_2)C_6H_4\}(PMe_2Ph)_3]PF_6$ (**4**) in which the added proton bridges the metal atom and a terminal methylene group. Crystals of **2** are monoclinic, space group $P2_1/n$, with a = 18.884 (3) Å, b = 18.612 (3) Å, c = 12.361 (1) Å, β = 90.40 (1)°, and Z = 4; those of **3** are monoclinic, space group $C2/c$, with a = 21.220 (8) Å, b = 23.412 (10) Å, c = 18.580 (7) Å, β = 126.05 (1)°, and Z = 8. The structures were solved by heavy-atom methods and refined by least-squares analysis to R = 0.042 and R_w = 0.053 for 5787 independent reflections ($I \geq 3\sigma$) (**2**) and R = 0.053 and R_w = 0.076 for 5832 independent reflections ($I > 3\sigma$) (**3**). Both cations contain a ruthenium atom coordinated in a distorted-octahedral arrangement by a η^3-pentamethylbenzyl group, which occupies two sites, three phosphorus atoms, and an agostic methyl hydrogen atom that has been directly located in **2** but not **3**. The η^3-benzyl interaction in **2** shows the usual asymmetry, the shortest Ru–C bond being to the terminal CH_2 group (Ru–C(22) = 2.164 (5) Å, Ru–C(2) = 2.342 (4) Å, Ru–C(1) = 2.358 (4) Å). The metrical parameters defining the agostic Ru–H–CH_2 interaction in **2** are r(Ru–C) = 2.416 (5) Å, r(Ru–H) = 1.92 (4) Å, r(C–H) = 1.01 (5) Å, and ∠C–H–Ru = 107 (3)°. The distances from ruthenium to the terminal carbon atoms in **3** (Ru–C(11) = 2.333 (9) Å, Ru–C(22) = 2.283 (10) Å) are almost equal within experimental error, in contrast with the corresponding distances in **2**, and indicate that the solid-state structure of **3** is an average in which either C(11) or C(22) is protonated. Variable-temperature NMR (^1H, ^{31}P) spectra of complexes **1**, **2**, **2a**, **3**, **3a**, and **4** show these molecules to be fluxional as a consequence of three processes: (1) reversible Ru–H (agostic) bond breaking, which cannot be frozen out, even at −100 °C; (2) reversible $\eta^3 \rightleftarrows \eta^1$ interconversions of the benzyl group, for which the estimated $\Delta G^{\ddagger}$ values are ca. 13 kcal/mol at 303 K for **2** and ca. 10 kcal/mol at 243 K for **3**; (3) reversible C–H bond breaking in the Ru–H–CH_2 bond, for which limiting high-temperature spectra cannot be reached owing to sample decomposition. For complexes **1**–**3**, a combination of these processes enables the RuL_3 fragment to circumnavigate the six-membered ring.

Introduction

o-Xylylene (*o*-quinodimethane) is a well-established example of a short-lived, unsaturated organic molecule that can be stabilized by coordination to a transition metal. Various bonding modes have been recognized (Figure 1). The molecule can bind as a two-electron σ-donor ligand via the exocyclic methylene groups, either to one metal atom (I), as in the complexes $Pt\{(CH_2)_2C_6H_4\text{-}o\}(1,5\text{-COD})$,[3] $M(\eta\text{-}C_5H_5)_2\{(CH_2)_2C_6H_4\text{-}o\}$ (M = Ti, Zr, Hf)[4] and $W\{(CH_2)_2C_6H_4\text{-}o\}_3$,[5] or to two metal atoms (II), as in the complexes $Co_2(\eta\text{-}C_5H_5)_2\{\mu\text{-}CO\}_2\{\mu\text{-}(CH_2)_2C_6H_4\text{-}o\}$[6] and $Pt_2Br_2Me_4\{\mu\text{-}(CH_2)_2C_6H_4\}(\mu\text{-}Ph_2PCH_2PPh_2)\}$.[7] *o*-Xylylene can also bind as a η^4-conjugated diene to low-valent transition-metal atoms, either via the exocyclic double bonds (III), as in $ML_3\{o\text{-}(CH_2)_2C_6H_4\}$ (M = Fe, Ru; L = CO, PR_3)[8-12] and $Co(\eta\text{-}C_5H_5)\{o\text{-}(CH_2)_2C_6H_4\}$,[4] or via the endo-

(1) On leave from the Department of Chemistry, University of Malaya, Kuala Lumpur, Malaysia.
(2) On leave from the School of Chemistry, The Queen's University of Belfast, Belfast, Northern Ireland.
(3) Lappert, M. F.; Martin, T. R.; Raston, C. L.; Skelton, B. W.; White, A. H. *J. Chem. Soc., Dalton Trans.* **1982**, 1159.
(4) Bristow, G. S.; Lappert, M. F.; Martin, T. R.; Atwood, J. L.; Hunter, W. F. *J. Chem. Soc., Dalton Trans.* **1984**, 399.
(5) Lappert, M. F.; Raston, C. L.; Rowbottom, G. L.; Skelton, B. W.; White, A. H. *J. Chem. Soc., Dalton Trans.* **1984**, 883.
(6) (a) Hersh, W. H.; Hollander, F. J.; Bergman, R. G. *J. Am. Chem. Soc.* **1983**, *105*, 5834. (b) Hersh, W. H.; Bergman, R. G. *J. Am. Chem. Soc.* **1983**, *105*, 5846.
(7) Hutton, A. T.; Shabanzadeh, B.; Shaw, B. L. *J. Chem. Soc., Chem. Commun.* **1982**, 1345.
(8) Roth, W. R.; Meier, J. D. *Tetrahedron Lett.* **1967**, 2053.

0276-7333/92/2311-3069$03.00/0

Scheme I

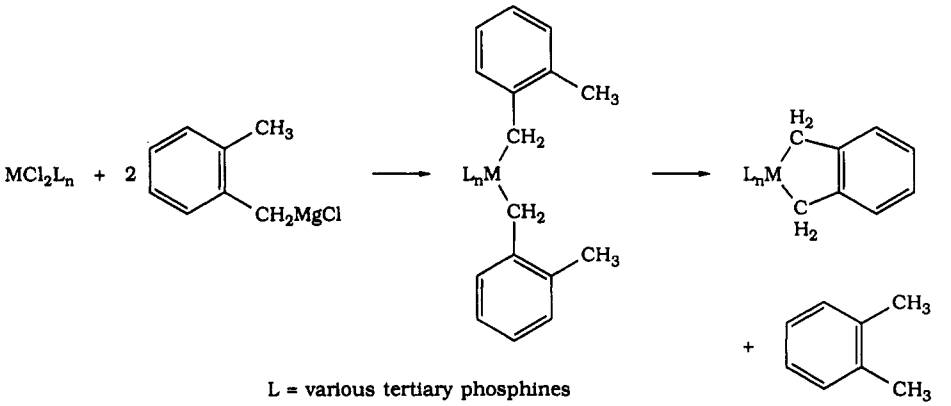

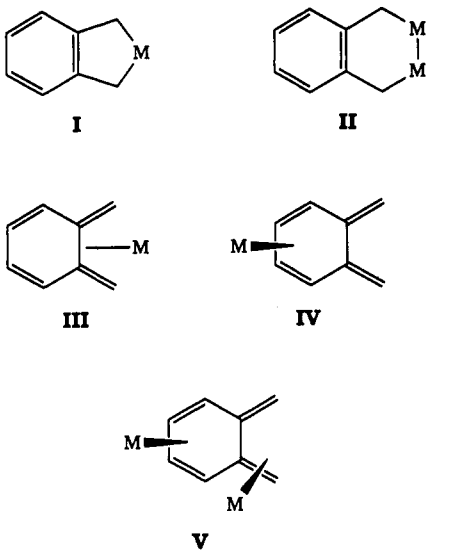

Figure 1. Bonding modes in (*o*-xylylene)metal complexes.

cyclic double bonds (IV), as in $M(\eta\text{-}C_6Me_6)\{o\text{-}(CH_2)_2C_6Me_4\}$ (M = Fe, Ru).[13,14] In the dinuclear complex $\{Ti(\eta\text{-}C_6Me_5)Cl\}_2\{\mu\text{-}o\text{-}(CH_2)_2C_6H_4\}$ the *o*-xylylene fragment bridges a pair of titanium atoms via both pairs of double bonds (V).[15]

o-Xylylene complexes are generally made from 1,2-bis(halomethyl) arenes (*o*-xylylene dihalides), either by direct reaction with a low-valent metal complex such as a metal carbonyl or metal carbonyl anion[6,8,9] or, more commonly, by reaction of the derived Grignard reagent with an appropriate metal halide.[3-5,7] A useful modification of the second method, which is particularly applicable to the later transition metals, employs the Grignard reagent of an *o*-methylbenzyl halide (Scheme I). In the case of iron and ruthenium, the intermediate bis(*o*-methylbenzyl) complexes cannot be detected, because they undergo spontaneous loss of *o*-xylene and form the *o*-xylylene complexes directly.[10,12] Naturally, the metal atom in the resulting mononuclear compounds is usually bound, in whatever fashion, to the *exo*-methylene groups.

Complexes in which the metal atom is attached to the *endo*-diene unit can be made from metal complexes containing a η^6-*o*-xylene derivative. Thus, the salt $[Ru(\eta^6\text{-}C_6Me_6)_2](PF_6)_2$ is deprotonated by potassium *tert*-butoxide to give $Ru(\eta^6\text{-}C_6Me_6)\{\eta^4\text{-}(CH_2)_2C_6Me_4\}$, which contains tetramethyl-*o*-xylylene (1,2-bis(methylene)-3,4,5,6-tetramethyl-2,5-cyclohexadiene) bound to zerovalent ruthenium via its endo double bonds (eq 1).[13]

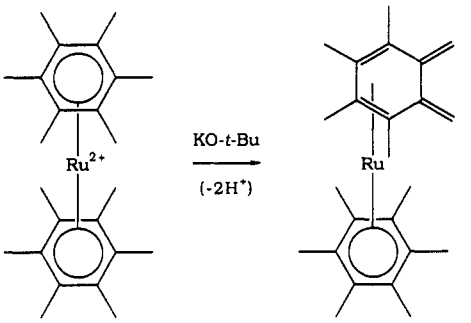

(1)

The analogous iron compound cannot be obtained by deprotonation of $[Fe(\eta^6\text{-}C_6Me_6)_2](PF_6)_2$, but reaction of the zerovalent iron complex $Fe(\eta^6\text{-}C_6Me_6)_2$ with dioxygen at −40 °C causes abstraction of two hydrogen atoms and formation of the *endo*-diene complex $Fe(\eta^6\text{-}C_6Me_6)\{\eta^4\text{-}(CH_2)_2C_6Me_4\}$.[14]

In a preliminary note,[16] we reported that, in contrast to the behavior of $[Ru(\eta^6\text{-}C_6Me_6)_2]^{2+}$, deprotonation of bis(tertiary phosphine)(η^6-hexamethylbenzene)ruthenium(II) complexes of the type $[Ru(ONO_2)(\eta^6\text{-}C_6Me_6)L_2]NO_3$ in the presence of another P-donor (L′) gives *exo*-η^4-tetramethyl-*o*-xylylene complexes of ruthenium(0), $Ru\{\eta^4\text{-}(CH_2)_2C_6Me_4\}L_2L'$; we also mentioned the protonation of some of these complexes. We present here a detailed account of our work on these systems.

Experimental Section

The following instruments were used: Varian HA100, JEOL MH100 (^{1}H NMR), JEOL FX60 (^{13}C at 15.0 MHz) Bruker CXP 200 (^{1}H NMR, ^{13}C NMR at 50.3 MHz, ^{31}P NMR at 81.0 MHz), Bruker B-KR 322S (^{31}P at 24.3 MHz), Bruker HFX 270 (^{1}H NMR at 270 MHz), MS 902 or VG Micromass 7070 F (mass spectra at 70 eV), Perkin-Elmer 683 (infrared), WTW LFD 550 (conductivity), and Knauer vapor pressure osmometer (molecular weights at 37 °C). All reactions were carried out under high-purity nitrogen or argon with use of standard Schlenk-tube, inert-atmosphere techniques. Elemental analyses were carried out in house; those for the *o*-xylylene complexes and their protonation products are in Table I. NMR data for the *o*-xylylene complexes are in Table II. The numbering used to describe the NMR spectra (^{1}H,

(9) Johnson, B. F. G.; Lewis, J.; Thompson, D. J. *Tetrahedron Lett.* **1974**, 3789.
(10) Chappell, S. D.; Cole-Hamilton, D. J.; Galas, A. M. R.; Hursthouse, M. B. *J. Chem. Soc., Dalton Trans.* **1982**, 1867.
(11) Simpson, N. J.; Cole-Hamilton, D. J. *J. Chem. Soc., Dalton Trans.* **1990**, 1329.
(12) Grosselin, J.-M.; Le Bozec, H.; Moinet, C.; Toupet, L.; Köhler, F. H.; Dixneuf, P. H. *Organometallics* **1988**, *7*, 88.
(13) Hull, J. W., Jr.; Gladfelter, W. L. *Organometallics* **1982**, *1*, 1716
(14) Madonik, A.; Astruc, D. *J. Am. Chem. Soc.* **1984**, *106*, 2437.
(15) Mena, M.; Royo, P.; Serrano, R.; Pellinghelli, M.; Tiripicchio, A. *Organometallics* **1988**, *7*, 258.
(16) Bennett, M. A.; McMahon, I. J.; Turney, T. W. *Angew. Chem., Int. Ed. Engl.* **1982**, *21*, 379; *Angew. Chem., Suppl.* **1982**, 853.

Table I. Analytical Data for (*o*-Xylylene)ruthenium(0) Complexes and Their Protonation Products

complex	% calcd			% found		
	C	H	P	C	H	P
Ru{η^4-$(CH_2)_2C_6Me_4$}{$P(OMe)_3$}$_3$[a]	39.8	6.85	14.7	40.1	6.9	14.6
Ru{η^4-$(CH_2)_2C_6Me_4$}{$P(OCH_2)_3CMe$}$_3$[b]	46.0	6.1		46.1	6.3	
Ru{η^4-$(CH_2)_2C_6Me_4$}$(PMe_2Ph)_3$[c]	64.0	7.3	13.75	64.25	7.3	13.8
Ru{η^4-$(CH_2)_2C_6Me_4$}$(Ph_2PCH_2CH_2PPh_2)(PMe_2Ph)$	69.2	6.5	11.65	68.5	6.5	11.4
Ru{η^4-$(CH_2)_2C_6Me_4$}{(*Z*)-$Ph_2PCH{=}CHPPh_2$}(PMe_2Ph)	69.4	6.2	11.7	69.5	6.35	11.2
Ru{η^4-$(CH_2)_2C_6Me_4$}$(PMePh_2)_3$	71.1	6.4		71.2	6.6	
Ru{η^4-$(CH_2)_2C_6H_2Me_2$}$(PMe_2Ph)_3$	63.05	7.0		63.0	7.1	
Ru{η^4-$(CH_2)_2C_6H_2Me_2$}$(PMePh_2)_3$	70.6	6.2		70.3	6.5	
Ru{η^4-$(CH_2)_2C_6H_4$}$(PMe_2Ph)_3$	62.0	6.7	15.0	62.05	6.8	15.1
[Ru{η^3-$(HCH_2)(CH_2)C_6Me_4$}$(Ph_2PCH_2CH_2PPh_2)(PMe_2Ph)$]$PF_6$ (1)	58.5	5.55	13.1	58.9	5.7	13.4
[Ru{η^3-$(HCH_2)(CH_2)C_6Me_4$}{(*Z*)-$Ph_2CH{=}CHPPh_2$}(PMe_2Ph)]PF_6 (2)	58.7	5.35		58.35	5.4	
[Ru{η^3-$(HCH_2)(CH_2)C_6Me_4$}{(*Z*)-$Ph_2PCH{=}CHPPh_2$}{$P(CD_3)_2Ph$}]PF_6 (2a)[d]	58.3	5.3[e]	13.1	57.7	5.5[e]	12.8
[Ru{η^3-$(HCH_2)(CH_2)C_6Me_4$}$(PMe_2Ph)_3$]PF_6 (3)[f]	52.6	6.1	15.1	52.6	6.1	14.9
[Ru{η^3-$(HCH_2)(CH_2)C_6Me_4$}{$P(CD_3)_2Ph$}$_3$]PF_6 (3a)	51.5	6.0[e]	14.8	51.25	5.9[e]	15.0
[Ru{η^3-$(HCH_2)(CH_2)C_6H_4$}$(PMe_2Ph)_3$]PF_6 (4)[g]	50.3	5.4	14.9 (F)	47.8	5.6	14.2 (F)
[Ru{η^6-C_6Me_6}$(PMe_2Ph)_3$]$(CF_3SO_3)_2$[h]	46.8	5.3	9.5	45.6	5.3	9.95

[a] Mass spectrum: m/z 634 (parent ion). [b] Mass spectrum: m/z 706 (parent ion). [c] Mass spectrum: m/z 676 (parent ion). [d] % F calcd 12.0, found 11.8. [e] H + D. [f] % F calcd 21.4, found 20.7. [g] Calcd for $4{\cdot}2H_2O$: C, 47.9; H, 5.8; F, 14.2. [h] % F calcd 11.7, found 12.4; % S calcd 6.6, found 6.65; % Ru calcd 10.4, found 10.2.

Table II. ^1H and $^{31}P\{^1H\}$ NMR Data for *o*-Xylylene Complexes of Ruthenium(0)[a,b]

	measd freq (^1H, ^{31}P)	^1H NMR				^{31}P NMR
		H^1	H^2	*o*-xylylene Me	ligand	
Ru{η^4-$(CH_2)_2C_6Me_4$}{$P(OMe)_3$}$_3$[c]	100, 24.3	0.23 (m)	2.54 (m)	2.42 (s), 2.19 (s)	3.65 (d, 9 H, J_{PH} = 11.5 Hz, OMe), 3.25 (m, 18 H, OMe)	175.7 (t, 1 P), 154.4 (d, 2 P, J_{PP} = 34 Hz)
Ru{η^4-$(CH_2)_2C_6Me_4$}{$P(OCH_2)_3CMe$}$_3$	100, 24.3	0.64 (m)	3.22 (m)	2.66 (s), 2.40 (s)	3.92 (d, 6 H, J_{PH} = 4.5 Hz), 3.72 (m, 18 H, CH_2), −0.14 (s, 9 H, CMe)	150.5 (t, 1 P), 128.5 (d, 2 P, J_{PP} = 39 Hz)
Ru{η^4-$(CH_2)_2C_6Me_4$}$(PMe_2Ph)_3$	270, 81.0	−0.22 (m)	2.33 (m)	2.25 (s), 2.22 (s)	1.85 (d, 6 H, J_{PH} = 7 Hz, PMe_2), 1.31 (vt, 6 H, *N* = 4 Hz, P*Me*Me), 1.19 (vt, 6 H, *N* = 4 Hz, PMe*Me*)	24.8 (t, 1 P), 3.1 (d, 2 P, J_{PP} = 3 Hz)
Ru{η^4-$(CH_2)_2C_6Me_4$}$(PMePh_2)_3$	200, 24.3	0.23 (m)	2.37 (m)	2.19 (s), 2.16 (s)	2.16 (d, J_{PH} ca. 7 Hz, PMe), 1.47 (vt, 6 H, *N* = 4 Hz, PMe)	35.9 (t, 1 P), 15.4 (d, 2 P, J_{PP} = 2 Hz)
Ru{η^4-$(CH_2)_2C_6Me_4$}$(Ph_2PCH_2CH_2)PPh_2)(PMe_2Ph)$	100, 24.3	−0.42 (m)	2.79 (m)	2.52 (s), 1.95 (s)	1.34 (m, 4 H, PCH_2), 1.14 (d, 6 H, J_{PH} = 8 Hz, PMe)	56.4 (br, 2 P, dppe), 19.0 (br, 1 P, PMe_2Ph) (J_{PP} < 2 Hz)
Ru{η^4-$(CH_2)_2C_6Me_4$}$(Ph_2PCH{=}CHPPh_2)(PMe_2Ph)$	200, 24.3	−0.15 (m)	2.91 (m)	2.35 (s), 2.02 (s)	1.11 (d, 6 H, J_{PH} = 8 Hz, PMe)	60.1 (s, 2 P, vdpp), 19.3 (s, 1 P, PMe_2Ph)
Ru{η^4-$(CH_2)_2C_6H_2Me_2$}$(PMe_2Ph)_3$	200, 24.3	−0.02 (m)	2.03 (m)	2.30 (s, 6 H)	1.90 (d, 6 H, J_{PH} = 7.5 Hz, PMe_2), 1.45 (vt, 6 H, *N* = 4 Hz, P*Me*Me), 1.35 (vt, 6 H, *N* = 4 Hz, *Me*)	24.6 (s, 1 P), 5.9 (s, 2 P)
Ru{η^4-$(CH_2)_2C_6H_2Me_2$}$(PMePh_2)_3$	100, 24.3	0.63 (m)	1.85 (m)	2.04 (s, 6 H)	2.12 (d, 3 H, J_{PH} = 7 Hz, PMe), 1.61 (vt, 6 H, *N* = 4 Hz, PMe)	34.3 (t, 1 P), 20.5 (d, 2 P, J_{PP} = 2 Hz)
Ru{η^4-$(CH_2)_2C_6H_4$}$(PMe_2Ph)_3$[d]	200, 81.0	−0.26 (dd, *J* = 7, 4 Hz)	1.81 (dd, *J* = 6, 4 Hz)	6.68 (m)[e]	1.65 (d, 6 H, J_{PH} = 7.6 Hz, PMe_2), 1.18 (vt, 6 H, *N* = 5.5 Hz), 1.11 (vt, 6 H, *N* = 5.5 Hz)	26.9 (d, 1 P), 6.1 (d, 2 P, J_{PP} = 3.5 Hz)

[a] In C_6D_6 (^1H) or C_6H_6 (^{31}P) at 20 °C, except where stated; all resonances in δ (ppm). [b] Abbreviations: vt = virtual triplet; $N = {}^2J_{PH} + {}^4J_{PH}$; dppe = $Ph_2PCH_2CH_2PPh_2$; vdpp = $Ph_2PCH{=}CHPPh_2$. [c] $^{13}C\{^1H\}$ NMR (15 MHz, C_6D_6) δ 133.3, 130.9 (C*Me*), 102.1 (*C*=CH_2), 50.8 (m, OMe), 26.2 (t, J_{PC} = 21 Hz, =CH_2), 17.4, 17.1 (C*Me*). [d] ^1H NMR (200 MHz, CD_2Cl_2) δ −0.78 (dd, *J* = 4, 2 Hz, H^1), 1.52 (dd, *J* = 5, 4 Hz, H^2), 1.80 (d, J_{PH} = 7.7 Hz, PMe_2Ph), 1.26 (vt, *N* = 5.7 Hz, P*Me*MePh), 1.19 (vt, *N* = 5.6 Hz, PMe*Me*Ph). [e] C_6H_4.

^{13}C, ^{31}P) of the protonation products is shown in Chart I in the Results. The compounds $P(OCH_2)_3CMe$,[17] $[RuCl_2(\eta^6\text{-arene})]_2$ (arene = 1-Me-4-$Me_2CHC_6H_4$, C_6Me_6),[18] and $Na[N(SiMe_3)_2]$[19] were made by the appropriate literature procedures, and commercial potassium *tert*-butoxide was freshly sublimed before use.

Preparations. Bis(μ-chloro)bis{chloro(η^6-*o*-xylene)ruthenium(II)}, $[RuCl_2(\eta^6\text{-}o\text{-}C_6H_4Me_2)]_2$. A mixture of hydrated $RuCl_3$ (2 g) and 1,2-dimethyl-1,4-cyclohexadiene (4 mL) in ethanol (20 mL) was heated under reflux for 2 h. The dark brown solid that separated on cooling was washed successively with methanol and ether and air-dried. The yield of $[RuCl_2(\eta^6\text{-}o\text{-}C_6H_4Me_2)]_2$ was 2.1–2.3 g (ca. 90–95%). ^1H NMR (100 MHz, DMSO-d_6): δ 5.74 (s, C_6H_4), 2.03 (s, Me). Anal. Calcd for $C_8H_{10}Cl_2Ru$: C, 34.5; H, 3.6. Found: C, 34.5; H, 3.6.

Bis(μ-chloro)bis{chloro(η^6-durene)ruthenium(II)}, $[RuCl_2(\eta^6\text{-}1,2,4,5\text{-}C_6H_2Me_4)]_2$. A mixture of $[RuCl_2(\eta^6$-1-Me-4-$Me_2CHC_6H_4)]_2$ (1.00 g, 1.63 mmol) and durene (10 g) was heated under reflux for 4 h. When it reached room temperature, the mixture was taken up in chloroform (ca. 50 mL) and filtered through Celite. The chloroform was removed by evaporation under reduced pressure, and the excess durene was removed from the residue by washing with pentane. The product was a brown solid (0.92 g, 92%). ^1H NMR (100 MHz, $CDCl_3$): δ 5.02 (s, C_6H_2), 2.08 (s, Me). Anal. Calcd for $C_{10}H_{14}Cl_2Ru$: C, 39.2; H, 4.6; Cl, 23.2. Found: C, 39.1; H, 4.5; Cl, 23.7.

Chloro(dimethylphenylphosphine)methyl(η^6-*o*-xylene)ruthenium(II), RuMeCl(η^6-*o*-$C_6H_4Me_2$)(PMe_2Ph). A suspension of $[RuCl_2(\eta^6\text{-}o\text{-}C_6H_4Me_2)]_2$ (0.50 g, 1.80 mmol) in acetonitrile (50 mL) was treated with tetramethyltin (1.5 mL), and the mixture was stirred for 16 h. Dimethylphenylphosphine (0.29 mL, 2.00 mL) was added, and stirring was continued for ca. 1 h. The solution was then chromatographed on neutral alumina. Acetonitrile eluted a yellow band which gave the product as a yellow oil; this slowly solidified but could not be crystallized. The yield was 0.37 g (52%). ^1H NMR (100 MHz, $CDCl_3$): δ 7.9–7.3 (m, Ph), 4.97 (d, *J* = 5 Hz, 1 H), 4.72 (s, 2 H), 4.64 (d, *J* = 5 Hz, 1 H) (C_6H_4), 1.92 (s), 1.81 (s), (C_6Me_2), 1.70 (d, J_{PH} = 9 Hz, P*Me*Me), 1.53 (d,

(17) Heitsch, C. W.; Verkade, J. G. *Inorg. Chem.* **1962**, *1*, 392.
(18) Bennett, M. A.; Huang, T.-N.; Matheson, T. W.; Smith, A. K. *Inorg. Synth.* **1982**, *21*, 74.
(19) Wannagat, U.; Niederprüm, H. *Chem. Ber.* **1961**, *94*, 1540.

J_{PH} = 9 Hz, PMe*Me*), 0.78 (d, J_{PH} = 8 Hz, RuMe).

The corresponding durene complex RuMeCl(η^6-*o*-$C_6H_2Me_4$)(PMe_2Ph) was prepared similarly and was recrystallized from dichloromethane/ether (39% yield). ^1H NMR (100 MHz, $CDCl_3$): δ 7.5–7.2 (m, Ph), 4.47 (d, J_{PH} = 2 Hz, C_6H_2), 1.70 (s), 1.60 (s) (C_6Me_4), 1.60 (d, J_{PH} = 7 Hz, P*Me*Me), 1.47 (d, J_{PH} = 7 Hz, PMe*Me*), 0.32 (d, J_{PH} = 8 Hz, RuMe). Anal. Calcd for $C_{19}H_{28}ClPRu$: C, 53.8; H, 6.7. Found: C, 53.7; H, 6.6.

Bis(dimethylphenylphosphine)methyl(*o*-xylene)ruthenium(II) Hexafluorophosphate, [RuMe(η^6-*o*-$C_6H_4Me_2$)(PMe_2Ph)$_2$]PF_6. A solution of RuMeCl(η^6-*o*-$C_6H_4Me_2$)(PMe_2Ph) (0.37 g, 0.94 mmol) in methanol (30 mL) was treated successively with PMe_2Ph (0.14 g, 1.01 mmol) and a solution of NH_4PF_6 (0.5 g) in water (0.6 mL). The mixture was stirred overnight and taken to dryness in vacuo. Extraction with dichloromethane, concentration of the filtered extract, and addition of ether gave the product as a pale yellow-brown solid (0.45 g, 74%). ^1H NMR (270 MHz, $CDCl_3$): δ 7.5–7.3 (m, Ph), 5.83 (m), 4.69 (m) (C_6H_4), 1.62 (virt t, $^2J_{PH} + {}^4J_{PH}$ = 9.3 Hz, P*Me*Me), 1.56 (s, C_6Me_2), 1.43 (virt t, $^2J_{PH} + {}^4J_{PH}$ = 9.5 Hz, PMe*Me*), 0.18 (t, J_{PH} = 6.3 Hz, RuMe). $^{31}P\{^1H\}$ NMR (24.3 MHz, $CHCl_3$): δ 13.0 (s, PMe_2Ph), −144.2 (spt, J_{PF} = 713 Hz, PF_6). Anal. Calcd for $C_{25}H_{35}P_3F_6Ru$: C, 46.7; H, 5.5; P, 14.4. Found: C, 46.6; H, 5.5; P, 14.8.

(η^6-Hexamethylbenzene)bis(nitrato)ruthenium(II), Ru(NO_3)$_2$(η^6-C_6Me_6). A mixture of [$RuCl_2$(η^6-C_6Me_6)]$_2$ (370 mg, 0.55 mmol) and silver nitrate (383 mg, 2.25 mmol) was stirred in acetone (20 mL) for 3 h at room temperature. The precipitated AgCl was removed by filtration, and the orange-brown solution was evaporated to dryness. Recrystallization of the residue from acetone/ether gave orange crystals of the product in ca. 80% yield. ^1H NMR (100 MHz, $CDCl_3$): δ 2.17 (s, C_6Me_6). IR (cm^{-1}, Nujol): 1495 (m), 1271 (s) (NO_3). Anal. Calcd for $C_{12}H_{18}N_2O_6Ru$: C, 37.2; H, 4.7; N, 7.2; mol wt, 387. Found: C, 37.4; H, 4.9; N, 7.0; mol wt, 390 (CH_2Cl_2), 198 ($MeNO_2$). Molar conductivity (Λ_M) in 10^{-3} M $MeNO_2$: 63 S cm^2 mol^{-1}.

The bis(nitrato)ruthenium(II) complexes of durene, mesitylene, *o*-xylene, and benzene were made similarly in 60–80% yield from the corresponding [$RuCl_2$(η^6-arene)]$_2$ complexes. *Caution*! The benzene compound is shock-sensitive.

Ru(NO_3)$_2$(η^6-1,2,4,5-$C_6H_2Me_4$): ^1H NMR (100 MHz, $CDCl_3$) δ 5.56 (s, C_6H_2), 2.23 (s, Me). Anal. Calcd for $C_{10}H_{14}N_2O_6Ru$: C, 33.4; H, 3.9; N, 7.8. Found: C, 33.3; H, 3.8; N, 7.6.

Ru(NO_3)$_2$(η^6-$C_6H_3Me_3$): ^1H NMR (100 MHz, $CDCl_3$) δ 5.34 (s, C_6H_3), 2.39 (s, Me); IR (cm^{-1}, Nujol) 1505 (s), 1271 (s) (NO_3). Anal. Calcd for $C_9H_{12}N_2O_6Ru$: C, 31.3; H, 3.5; N, 8.1. Found: C, 31.4; H, 3.6; N, 8.05.

Ru(NO_3)$_2$(η^6-1,2-$C_6H_4Me_2$): ^1H NMR (100 MHz, CD_2Cl_2) δ 5.84 (m, C_6H_4), 2.25 (s, Me); IR (cm^{-1}, Nujol) 1570 (m), 1525 (s), 1275 (s), 1230 (s), 990 (s) (NO_3). Anal. Calcd for $C_8H_{10}N_2O_6Ru$: C, 29.0; H, 3.0. Found: C, 29.0; H, 3.0.

Ru(NO_3)$_2$(η^6-C_6H_6): ^1H NMR (100 MHz, acetone-d_6) δ 6.27 (s, C_6H_6). Anal. Calcd for $C_6H_6N_2O_6Ru$: C, 23.8; H, 2.0; N, 9.2. Found: C, 24.0; H, 2.5; N, 9.0.

(η^6-Hexamethylbenzene)bis(nitrato)(triphenylphosphine)ruthenium(II), Ru(NO_3)$_2$(η^6-C_6Me_6)(PPh_3). A mixture of triphenylphosphine (554 mg, 2.11 mmol) and Ru(NO_3)$_2$(η^6-C_6Me_6) (414 mg, 1.07 mmol) in acetone (25 mL) was heated to 40 °C for 10 min. Addition of ether (150 mL) caused an orange solid to precipitate. Two recrystallizations from acetone/ether gave the product (581 mg, 83%). ^1H NMR (100 MHz, CD_2Cl_2): δ 7.46–7.36 (m, Ph), 1.85 (d, J_{PH} = 1.0 Hz, C_6Me_6). Anal. Calcd for $C_{30}H_{33}N_2O_6PRu$: C, 55.5; H, 5.1; N, 4.3; P, 4.75. Found: C, 55.3; H, 5.0; N, 4.1; P, 5.3.

(η^6-Hexamethylbenzene)bis(trimethyl phosphite)(nitrato)ruthenium(II) Nitrate, [Ru(ONO_2)(η^6-C_6Me_6){P(OMe)$_3$}$_2$]NO_3. An excess of trimethyl phosphite (2 mL) was added to a solution of Ru(NO_3)$_2$(η^6-C_6Me_6) (321 mg, 0.83 mmol). After a few minutes the color had become yellow. The solution was evaporated to dryness, and the residue was recrystallized from dichloromethane/ether to give the yellow, crystalline product (231 mg, 43%). ^1H NMR (100 MHz, CD_2Cl_2): δ 3.75 (virt t, $^2J_{PH} + {}^4J_{PH}$ = 5.0 Hz, OMe), 2.09 (t, J_{PH} = 1.2 Hz, C_6Me_6). Anal. Calcd for $C_{18}H_{36}N_2O_6P_2Ru$: C, 34.0; H, 5.2; N, 4.4; P, 9.6. Found: C, 34.15; H, 5.8; N, 4.2; P. 9.7.

The complex [Ru(ONO_2)(η^6-C_6Me_6){P(OCH_2)$_3$CMe}$_2$]NO_3 was prepared similarly in 60% yield from Ru(NO_3)$_2$(η-C_6Me_6) and P(OCH_2)$_3$CMe. ^1H NMR (100 MHz, $CDCl_3$): δ 4.46 (m, CH_2), 2.22 (s, C_6Me_6), 0.91 (s, CMe). $^{31}P\{^1H\}$ NMR (24.3 MHz, $CHCl_3$): δ 145.0. IR (cm^{-1}, Nujol): 1495, 1270 (NO_3). Anal. Calcd for $C_{22}H_{36}N_2O_{12}P_2Ru$: C, 38.65; H, 5.3; N, 4.1. Found: C, 38.3; H, 5.1; N, 4.0.

(η^6-Hexamethylbenzene){1,2-bis(diphenylphosphino)ethane}(nitrato)ruthenium(II) Nitrate, [Ru(ONO_2)(η^6-C_6Me_6)(dppe)]NO_3. A solution of dppe (366 mg, 0.92 mmol) in dichloromethane (10 mL) was added to a solution of Ru(NO_3)$_2$(η^6-C_6Me_6) (356 mg, 0.92 mmol) in acetone (40 mL), and the mixture was set aside for 30 min. The yellow precipitate that formed on addition of hexane (200 mL) was collected and recrystallized twice from dichloromethane/ether to give the product as a dichloromethane solvate (194 mg, 26%). ^1H NMR (100 MHz, CD_2Cl_2): δ 7.4 (m, Ph), 2.98 (m, CH_2), 1.77 (t, J_{PH} = 0.8 Hz, C_6Me_6). Anal. Calcd for $C_{38}H_{42}N_2O_6P_2Ru{\cdot}0.3CH_2Cl_2$: C, 56.6; H, 5.3; N, 3.4; P, 7.6; Cl, 2.9. Found: C, 56.55; H, 5.4; N, 3.2; P, 8.1; Cl, 2.8.

(η^6-Hexamethylbenzene)bis(dimethylphenylphosphine)(nitrato)ruthenium(II) Nitrate, [Ru(ONO_2)(η^6-C_6Me_6)(PMe_2Ph)$_2$]NO_3. Dimethylphenylphosphine (143 mg, 1.04 mmol) was added to a solution of Ru(NO_3)$_2$(η^6-C_6Me_6) (200 mg, 0.52 mmol) in acetone (10 mL), and the mixture was set aside for 30 min. The solution was evaporated to dryness under reduced pressure, and the residue was recrystallized from dichloromethane/pentane to give the product as a yellow, air-sensitive solid (190 mg, 55%). ^1H NMR (100 MHz, CD_2Cl_2): δ 7.8–7.4 (m, Ph), 1.86 (s, C_6Me_6), 1.75 (m, P*Me*MePh), 1.57 (m, PMe*Me*Ph). $^{31}P\{^1H\}$ NMR (24.3 MHz, CH_2Cl_2): δ 8.5. Anal. Calcd for $C_{28}H_{40}N_2O_6P_2Ru$: C, 50.8; H, 5.8; N, 8.5; P, 9.4. Found: C, 50.45; H, 6.0; N, 8.4; P, 9.1.

Preparation of [Ru(O_2CCF_3)(η^6-arene)L_2]PF_6 Complexes. Method 1. A mixture of [$RuCl_2$(η^6-C_6Me_6)]$_2$ (2.0 g, 2.99 mol) and silver acetate (2.0 g, 12.0 mmol) was stirred for 18 h in benzene (300 mL). The resulting solution was filtered through Celite to remove AgCl, solvent was removed under reduced pressure, and the residual solid was treated with trifluoroacetic acid (16 mL) for 30 min. The excess acid was removed under reduced pressure, and the residue was dissolved in methanol (60 mL). Addition of PMe_2Ph (1.74 mL, 12.0 mmol) gave a red solution which, when treated with a solution of NH_4PF_6 (7.2 g) in water (6 mL), deposited a yellow solid. This was collected by filtration, washed with water, dried in vacuo, and extracted with dichloromethane (ca. 15 mL). The filtered extract was concentrated under reduced pressure. Adding ether and cooling to 0 °C gave [Ru(O_2CCF_3)(η^6-C_6Me_6)(PMe_2Ph)$_2$]PF_6 as a yellow solid (3.9 g, 82% yield). ^1H NMR (CD_2Cl_2, 100 MHz): δ 7.8–7.5 (m, Ar), 1.74 (s, C_6Me_6), 1.74 (virt t, $^2J_{PH} + {}^4J_{PH}$ = 10 Hz, P*Me*Me), 1.48 (virt t, $^2J_{PH} + {}^4J_{PH}$ = 11 Hz, PMe*Me*). $^{31}P\{^1H\}$ NMR (CH_2Cl_2, 24.3 MHz): 9.85 (s, PMe_2Ph), −144.8 (spt, J_{PF} = 710 Hz, PF_6). Anal. Calcd for $C_{30}H_{40}O_2F_9P_3Ru$: C, 45.2; H, 5.05; F, 21.4; P, 11.65. Found: C, 44.9; H, 5.2; F, 20.7; P, 11.9.

The following compounds were prepared similarly; yields are in parentheses.

[Ru(O_2CCF_3)(η^6-C_6Me_6)($PMePh_2$)$_2$]PF_6 (70%): ^1H NMR (CD_2Cl_2, 100 MHz) δ 7.8–6.8 (m, Ph), 1.76 (s, C_6Me_6), 1.28 (virt t, $^2J_{PH} + {}^4J_{PH}$ = 10 Hz, PMe). Anal. Calcd for $C_{40}H_{44}O_2F_9P_3Ru$: C, 52.1; H, 4.8. Found: C, 51.2; H, 4.8.

[Ru(O_2CCF_3)(η^6-C_6Me_6){(*Z*)-$Ph_2PCH{=}CHPPh_2$}]PF_6 (80%): ^1H NMR (CD_2Cl_2, 100 MHz) δ 7.8–7.0 (m, Ph, =CH), 1.73 (s, C_6Me_6). Anal. Calcd for $C_{40}H_{40}O_2F_9P_3Ru$: C, 52.35; H, 4.4 Found: C, 50.85; H, 4.3 (low carbon obtained even after two recrystallizations from CH_2Cl_2/ether).

[Ru(O_2CCF_3)(η^6-$C_6H_2Me_4$)(PMe_2Ph)$_2$]PF_6 (62%): ^1H NMR (CD_2Cl_2, 100 MHz) δ 7.9–7.5 (m, Ph), 5.36 (s, C_6H_2), 1.81 (virt t, $^2J_{PH} + {}^4J_{PH}$ = 10 Hz, P*Me*Me), 1.76 (s, C_6Me_4), 1.55 (virt t, $^2J_{PH} + {}^4J_{PH}$ = 10 Hz, PMe*Me*). Anal. Calcd for $C_{28}H_{36}O_2F_9P_3Ru$: C, 43.7; H, 4.7. Found: C, 44.0; H, 4.7.

[Ru(O_2CCF_3)(η^6-$C_6H_2Me_4$)($PMePh_2$)$_2$]PF_6 (69%): ^1H NMR (CD_2Cl_2, 100 MHz) δ 7.8–7.0 (m, Ph), 5.60 (s, C_6H_2), 1.67 (s, C_6Me_4), 1.38 (virt t, $^2J_{PH} + {}^4J_{PH}$ = 10 Hz, PMe). Anal. Calcd for $C_{38}H_{40}O_2F_9P_3Ru$: C, 51.1; H, 4.5. Found: C, 50.9; H, 4.6.

[Ru(O_2CCF_3)(η^6-$C_6H_2Me_4$){(*Z*)-$Ph_2PCH{=}CHPPh_2$}]PF_6 (84%): ^1H NMR (CD_2Cl_2, 100 MHz) δ 7.8–7.0 (m, Ph, =CH), 5.73 (s, C_6H_2), 1.63 (s, C_6Me_4). Anal. Calcd for $C_{38}H_{36}O_2F_9P_3Ru$: C, 51.3; H, 4.1. Found: C, 51.2; H, 4.0.

[Ru(O_2CCF_3)(η^6-*o*-$C_6H_4Me_2$)(PMe_2Ph)$_2$]PF_6 (59%): ^1H NMR (CD_2Cl_2, 100 MHz) δ 7.60 (br m, Ph), 5.53 (m), 5.30 (m) (C_6H_4), 1.76 (s, C_6Me_2), 1.75 (virt t, $^2J_{PH} + {}^4J_{PH}$ = 10 Hz, P*Me*Me), 1.58 (virt t, $^2J_{PH} + {}^4J_{PH}$ = 11 Hz, PMe*Me*); $^{31}P\{^1H\}$ NMR (CH_2Cl_2, 24.3 MHz) δ 9.85 (s, PMe_2Ph), −144.7 (spt, J_{PF} = 712 Hz, PF_6). Anal. Calcd for $C_{26}H_{32}O_2F_9P_3Ru$: C, 42.1; H, 4.35; P, 12.5. Found: C, 42.2; H, 4.3; P, 12.8.

[Ru(O_2CCF_3)(η^6-*o*-$C_6H_4Me_2$)($PMePh_2$)$_2$]PF_6 (63%): ^1H NMR (CD_2Cl_2, 100 MHz) δ 7.7–7.1 (m, Ph), 5.65 (m), 5.35 (m) (C_6H_4), 1.85 (s), 1.76 (s) (ca. 1:2 ratio, C_6Me_2), 1.64, 1.48 (each virt t, $^2J_{PH} + {}^4J_{PH}$ = 10 Hz, ca. 1:2 ratio, PMe); $^{31}P\{^1H\}$ NMR (CH_2Cl_2, 24.3 MHz) δ 14.9, 14.3 (each s, ca. 3:1 ratio, $PMePh_2$), −144.6 (spt, J_{PF} = 712 Hz, PF_6). Anal. Calcd for $C_{36}H_{36}O_2F_9P_3Ru$: C, 50.0; H, 4.2. Found: C, 49.9; H, 4.2.

[Ru(O_2CCF_3)(η^6-C_6H_6)(PMe_2Ph)$_2$]PF_6 (64%): ^1H NMR (CD_2Cl_2, 100 MHz) δ 7.65–7.30 (m, Ph), 5.73 (s, C_6H_6), 1.77 (virt t, $^2J_{PH} + {}^4J_{PH}$ = 10 Hz, P*Me*Me), 1.61 (virt t, $^2J_{PH} + {}^4J_{PH}$ = 10 Hz, PMe*Me*). Anal. Calcd for $C_{24}H_{28}O_2F_9P_3Ru$: C, 40.4; H, 4.0. Found: C, 40.4; H, 3.9.

Method 2. A sample of [RuMe(η^6-*o*-$C_6H_4Me_2$)(PMe_2Ph)$_2$]PF_6 (350 mg, 0.54 mmol) was stirred with CF_3CO_2H (3 mL) for 12 h. The excess acid was removed in vacuo, and the residue was stirred for 2 h with methanol (10 mL) and NH_4PF_6 (0.5 g). Solvent was removed under reduced pressure, and the residue was extracted with dichloromethane. Concentration of the extract and addition of ether gave pale yellow [Ru(O_2CCF_3)(*o*-$C_6H_4Me_2$)(PMe_2Ph)$_2$]PF_6 (314 mg, 78%).

Similar treatment of [RuMe(η^6-C_6H_6)(PMe_2Ph)$_2$]PF_6 gave [Ru(O_2CCF_3)(η^6-C_6H_6)(PMe_2Ph)$_2$]PF_6 in 62% yield.

Preparation of *o*-Xylylene Complexes. (1) Ru{η^4-$(CH_2)_2C_6Me_4$}{$P(OMe)_3$}$_3$. Trimethyl phosphite (1 mL) was added to a suspension of [Ru(ONO_2)(η^6-C_6Me_6){$P(OMe)_3$}$_2$]NO_3 (0.2 g, 0.3 mmol) in THF (25 mL). Potassium *tert*-butoxide (0.2 g, 1.8 mmol) was then added, and the mixture was stirred for 1 h, after which time the starting material had disappeared and a yellow solution had formed. The solvent was removed under vacuum, and the residue was extracted with *n*-pentane (40 mL). Evaporation of *n*-pentane gave the crude product as a yellow oil in ca. 70% yield. This was purified by chromatography in hexane on neutral alumina (activity 1). The eluate was concentrated under vacuum to ca. 2 mL and cooled to −78 °C to give the product as a yellow solid (0.02 mg, 10%).

Powdered KOH could also be used in place of KO-*t*-Bu, with similar results. Under the same conditions, $RuCl_2$(η^6-C_6Me_6){$P(OMe)_3$} and [RuCl(η^6-C_6Me_6){$P(OMe)_3$}$_2$]PF_6 did not react with KO-*t*-Bu.

(2) Ru{η^4-$(CH_2)_2C_6Me_4$}{$P(OCH_2)_3CMe$}$_3$. The complex [Ru(ONO_2)(η^6-C_6Me_6){$P(OCH_2)_3CMe$}$_2$]NO_3 (0.2 g, 0.37 mmol) was added to a solution of $P(OCH_2)_3CMe$ (0.056 g, 0.37 mmol) in THF (25 mL). Potassium *tert*-butoxide (0.2 g) was added, and the mixture was stirred for 1 h. Solvent was removed under vacuum, and the residue was extracted with benzene (100 mL). The extract was evaporated to dryness, and any unreacted $P(OCH_2)_3CMe$ was removed by sublimation at 60 °C/0.1 mm. The residue was washed with ether and redissolved in benzene. The filtered benzene solution was evaporated to dryness to give the product as a white solid (0.05 g, 20%).

(3) Ru{η^4-$(CH_2)_2C_6Me_4$}($Ph_2PCH_2CH_2PPh_2$)(PMe_2Ph). Dimethylphenylphosphine (0.036 g, 0.26 mmol) was added to a suspension of [Ru(ONO_2)(η^6-C_6Me_6)($Ph_2PCH_2CH_2PPh_2$)]NO_3 (0.2 g, 0.26 mmol) in THF (25 mL). Potassium *tert*-butoxide (0.2 g) was added, and the mixture was stirred for 1 h. After removal of solvent under vacuum, the residue was washed with hexane and extracted with benzene (30 mL). Evaporation of the benzene gave a yellow solid, which was washed with hexane to remove an unknown contaminant and dried under vacuum. The yield was 0.10 g (49%).

(4) Ru{η^4-$(CH_2)_2C_6Me_4$}(PMe_2Ph)$_3$. A solution of [Ru(O_2CCF_3)(η^6-C_6Me_6)(PMe_2Ph)$_2$]PF_6 (1.0 g, 1.25 mmol) in THF (100 mL) was treated successively with dimethylphenylphosphine (0.18 mL, 1.25 mmol) and potassium *tert*-butoxide (0.42 g, 3.75 mmol), and the mixture was stirred at room temperature for 2 h. The color changed from orange to lemon yellow. Solvents were removed under reduced pressure, and the solid residue was extracted with ether (6 × 10 mL). The extracts were filtered through neutral alumina, which removed a green impurity, and the lemon yellow filtrate was concentrated under vacuum to ca. 10 mL. Cooling in dry ice gave yellow crystals of Ru{η^4-$(CH_2)_2C_6Me_4$}-(PMe_2Ph)$_3$, which were separated by filtration and dried under vacuum. The yield was 0.67 g (79%).

The following compounds were prepared similarly from the appropriate [Ru(O_2CCF_3)(η^6-arene)L_2]PF_6 complexes, P-donor ligands, and KO-*t*-Bu; yields are in parentheses: Ru{η^4-$(CH_2)_2C_6Me_4$}{(*Z*)-Ph_2PCH=$CHPPh_2$}(PMe_2Ph) (80%), Ru{η^4-$(CH_2)_2C_6Me_4$}($PMePh_2$)$_3$ (85%), Ru{η^4-$(CH_2)_2C_6H_2Me_2$}(PMe_2Ph)$_3$ (37%), and Ru{η^4-$(CH_2)_2C_6H_2Me_2$}($PMePh_2$)$_3$ (44%). The compound Ru{η^4-$(CH_2)_2C_6H_2Me_2$}(PMe_2Ph)$_3$ was also made from [Ru(ONO_2)(η^6-$C_6H_2Me_4$)(PMe_2Ph)$_2$]NO_3, PMe_2Ph, and KO-*t*-Bu.

(5) Ru{η^4-$(CH_2)_2C_6H_4$}(PMe_2Ph)$_3$. To a suspension of [Ru(O_2CCF_3)(η^6-$C_6H_4Me_2$)(PMe_2Ph)$_2$]PF_6 (0.53 g, 0.71 mmol) in THF (80 mL) was added successively PMe_2Ph (0.16 mL, 1.07 mmol) and Na[$N(SiMe_3)_2$] (0.34 g, 1.85 mmol). The mixture was stirred at room temperature for 5 h, during which time the color changed from yellow to orange and finally to lemon yellow. Solvent was removed under vacuum, the residue was extracted with ether (5 × 10 mL), and the extracts were filtered through neutral alumina. The yellow filtrate was concentrated to ca. 2 mL, *n*-pentane (ca. 2 mL) was added, and the solution was set aside overnight at −78 °C. The yield of orange, crystalline product was 0.32 g (71%).

Similar reactions employing KO-*t*-Bu instead of Na[$N(SiMe_3)_2$] gave Ru{η^4-$(CH_2)_2C_6H_4$}(PMe_2Ph)$_3$ in 30–45% yield.

Protonation of *o*-Xylylene Complexes. (1) Aqueous 60% HPF_6 was added dropwise to a solution of Ru(η^4-$(CH_2)_2C_6Me_4$}($Ph_2PCH_2CH_2PPh_2$)(PMe_2Ph) (0.1 g, 0.13 mmol) in ether (50 mL). The yellow precipitate of Ru{η^3-(HCH_2)-$(CH_2)C_6Me_4$}($Ph_2PCH_2CH_2PPh_2$)(PMe_2Ph)]PF_6 (1) was separated by filtration, washed with ether, and dried under vacuum. The yield was 0.095 g (80%). ^1H NMR (100 MHz, CD_2Cl_2, −30 °C): δ 7.8–6.7 (m, Ph), 3.17 (m, H^5), 2.40 (s, Me^8), 2.17 (s, Me^6), 1.58 (s, Me^7 or Me^9), 1.42 (s, Me^9 or Me^7), 1.22 (d, J_{PH} = 10 Hz, PMe), 0.77 (d, J_{PH} = 9 Hz, PMe), −2.31 (m, $H^{1,2,3}$). ^1H NMR (100 MHz, $C_2H_4Cl_2$, 27 °C): 7.8–6.7 (m, Ph), 2.38 (s, Me^8), 1.87 (s, Me^7, Me^9), 1.02 (d, J_{PH} = 9 Hz, PMe), −0.20 (v br, $H^{1,2,3}$, Me^6). $^{31}P\{^1H\}$ NMR (24.3 MHz, CD_2Cl_2, −30 °C): δ 77.6 (dd, $Ph_2PCH_2CH_2PPh_2$), 49.1 (d, J_{PP} = 19.5 Hz, $Ph_2PCH_2CH_2PPh_2$), 14.4 (d, J_{PP} = 43.9 Hz, PMe_2Ph), −143.9 (sp, J_{PF} = 712 Hz, PF_6).

(2) A sample of Ru{η^4-$(CH_2)_2C_6Me_4$}{(*Z*)-Ph_2PCH=$CHPPh_2$}(PMe_2Ph) in ether (ca. 80 mL), which had been made directly, without isolation, from [Ru(O_2CCF_3)(η-C_6Me_6){(*Z*)-Ph_2PCH=$CHPPh_2$}]PF_6 (1.01 g, 1.10 mmol), PMe_2Ph (0.16 mL, 1.10 mmol), and KO-*t*-Bu (0.364 g, 3.25 mmol), was treated with aqueous 60% HPF_6 (0.80 mL, ca. 5.7 mmol). The orange precipitate was allowed to settle, filtered, washed with ether, and dried under vacuum. The yield of [Ru(η^3-(HCH_2)-$(CH_2)C_6Me_4$}{(*Z*)-Ph_2PCH=$CHPPh_2$}(PMe_2Ph)]PF_6 (**2**) was 0.68 g (66%). Orange crystals were obtained from 1:1 dichloromethane/ether at 0 °C. The corresponding $P(CD_3)_2Ph$ complex (**2a**) was obtained similarly in 74% yield. ^1H NMR of **2a** (270 MHz, CD_2Cl_2, −60 °C): δ 7.6–6.4 (Ph), 5.75 (dd, J_{HH} = 7.4 Hz, J_{PH} = 11.6 Hz, CH=CH), 3.24 (dd, J_{HH} = 5.7 Hz, J_{PH} = 1.4 Hz, H^5), 2.19 (s, Me^8), 1.97 (s, Me^6), 1.74 (s, Me^7 or Me^9), 1.62 (s, Me^9 or Me^7), 0.78 (d, J_{HH} = 5.9 Hz, H^4), −2.20 (br d, J_{PH} = 6 Hz, $H^{1,2,3}$). ^1H NMR (CD_2Cl_2, 0 °C): δ 7.7–6.4 (m, Ph), 5.9 (br, CH=CH), 3.14 (br s, H^5), 2.15 (s, Me^8), 1.92 (br s, Me^6), 1.65 (br s, Me^7, Me^9), 0.88 (br s, H^4), −2.02 (br s, $H^{1,2,3}$). $^{31}P\{^1H\}$ NMR (81.0 MHz, CD_2Cl_2, −55 °C) δ 84.9 (m, Ph_2PCH=$CHPPh_2$), 31.6 (m, PMe_2Ph), −143.9 (sp, J_{PF} = 712 Hz, PF_6). ^1H NMR of **2** (270 MHz, CD_2Cl_2, −60 °C): as for **2a**, with addition of δ 1.12 (d, J_{PH} = 8 Hz, PMe), 0.61 (d, J_{PH} = 10 Hz, PMe).

(3) Treatment of Ru{η^4-$(CH_2)_2C_6Me_4$}(PMe_2Ph)$_3$ (0.67 g, 0.99 mmol) with 60% HPF_6 (aqueous) and recrystallization of the resulting solid from dichloromethane/ether gave orange crystals of [Ru{η^3-$(HCH_2)(CH_2)C_6Me_4$}(PMe_2Ph)$_3$]PF_6 (**3**; 0.79 g, 96%). Single crystals suitable for X-ray diffraction analysis were obtained by dissolving a sample in hot methanol and setting the solution aside for 3 days. Molar conductivity Λ_M: 54 S cm^2 mol^{-1} (CH_2Cl_2), 80.5 S cm^2 mol^{-1} ($MeNO_2$). The corresponding $P(CD_3)_2Ph$ complex **3a** was obtained similarly. ^1H NMR of **3a** (270 MHz, CD_2Cl_2, −90 °C): δ 7.4–6.9 (m), 6.75 (t, J_{PH} = 8 Hz) (Ph), 2.7 (br, H^5), 2.2–1.9 (overlapping s, $Me^{6,7,8,9}$), 0.6 (br, H^4), −2.5 (br, $H^{1,2,3}$). ^1H NMR (270 MHz, CD_2Cl_2, −30 °C): δ 7.4–6.8 (br m, Ph), 2.26 (s, Me^8), 2.13 (s, Me^7, Me^9). ^1H NMR of **3** (270 MHz, CD_2Cl_2, −90

°C): as for **3a**, with addition of δ 1.31 (m, 2 PMe), 1.11 (t, sepn 8 Hz, 1 PMe). $^{31}P\{^1H\}$ NMR (81.0 MHz, CD_2Cl_2, −90 °C): δ 32.2 (dd), 20.7 (d, J_{PP} = 48.5 Hz), −8.25 (d, J_{PP} = 32.5 Hz), −143.9 (spt, J_{PF} = 712 Hz, PF_6). $^{31}P\{^1H\}$ NMR (81.0 MHz, CD_2Cl_2, 0 °C): δ 25.5 (br s, 2 P), −8.6 (br s, 1 P).

(4) Dropwise addition of 60% aqueous HPF_6 to a solution of $Ru\{\eta^4\text{-}(CH_2)_2C_6Me_4\}\{P(OMe)_3\}_3$ (0.1 g) in ether (10 mL) precipitated a white solid which was identified by ^1H NMR spectroscopy as $[Ru(\eta^6\text{-}C_6Me_6)\{P(OMe)_3\}_3](PF_6)_2$. ^1H NMR (100 MHz, CD_2Cl_2): δ 3.83 (m, OMe), 2.22 (s, C_6Me_6).

Dropwise addition of $HBF_4\cdot OEt_2$ (0.02 g, 0.12 mmol) in ether (30 mL) to a vigorously stirred solution of $Ru\{\eta^4\text{-}(CH_2)_2C_6Me_4\}\{P(OMe)_3\}_3$ (0.075 g, 0.12 mmol) in ether (30 mL) at 0 °C gave a pale yellow precipitate, which was shown by ^1H NMR spectroscopy to be a 1:1 mixture of $[Ru(\eta^6\text{-}C_6Me_6)\{P(OMe)_3\}_3](BF_4)_2$ and a monoprotonated cation, presumably $[Ru\{\eta^3\text{-}(HCH_2)(CH_2)C_6Me_4\}\{P(OMe)_3\}_3]BF_4$. ^1H NMR (100 MHz, CD_2Cl_2): δ 3.51 (q, J_{PH} = 3 Hz, OMe), 2.28 (s, Me^7, Me^9 (av)), 2.23 (s, Me^8), 1.76 (m, H^4, H^5 (av)), 0.12 (q, J_{PH} = 2.5 Hz, $H^{1,2,3}$, Me^6 (av)).

(5) A sample of $Ru\{\eta^4\text{-}(CH_2)_2C_6Me_4\}(PMe_2Ph)_3$ in ether (10 mL), which had been made directly, without isolation, from $[Ru(O_2CCF_3)(\eta\text{-}C_6Me_6)(PMe_2Ph)_2]PF_6$ (1.3 g, 1.6 mmol), was treated with CF_3SO_3H (0.24 mL, 2.6 mmol). The resulting orange-red solid, presumed to be $[Ru\{(\eta^3\text{-}HCH_2)(CH_2)C_6Me_4\}(PMe_2Ph)_3]CF_3SO_3$, was separated by filtration, washed with ether, and dissolved in methanol. Addition of more CF_3SO_3H (1.65 mL, 1.83 mmol) caused the color of the solution to change from orange to clear lemon yellow. Concentrating, adding ether (30 mL), and cooling to −78 °C gave $[Ru(\eta^6\text{-}C_6Me_6)(PMe_2Ph)_3](CF_3SO_3)_2$ (0.45 g, 28%) as a yellow solid. Λ_M in $MeNO_2$: 180 S cm^2 mol^{-1}. ^1H NMR (100 MHz, CD_3OD): δ 7.56 (m, Ph), 2.09 (s, C_6Me_6), 1.98 (virt t, sepn 9 Hz, PMe). This complex readily loses C_6Me_6 in solution over a period of 18 h at room temperature.

(6) Treatment of $[Ru\{\eta^4\text{-}(CH_2)_2C_6H_4\}(PMe_2Ph)_3]$ (0.10 g, 0.16 mmol) in ether (40 mL) with 60% aqueous HPF_6 gave an immediate yellow precipitate. This was filtered at 0 °C, washed with ether (5 × 10 mL), and dried under vacuum. The yield of crude $[Ru\{\eta^3\text{-}(HCH_2)(CH_2)C_6H_4\}(PMe_2Ph)_3]PF_6$ (**4**) was about 90%. Extraction with dichloromethane gave an orange solution and a small amount of undissolved solid, $[Ru(\eta^6\text{-}o\text{-}C_6H_4Me_2)(PMe_2Ph)_3](PF_6)_2$, which was removed by filtration. Addition of ether to the solution gave **4** as a fine yellow solid which was recrystallized from methanol/ether. ^1H NMR (270 MHz, CD_2Cl_2, −90 °C): δ 7.6–6.9 (m, Ar), 2.48 (d, J_{HH} = 5 Hz, H^5), 1.61 (br s, PMe), 0.75 (d, J_{HH} = 5 Hz, H^4), −2.38 (br s, $H^{1,2,3}$). $^{31}P\{^1H\}$ NMR (81.0 MHz, CD_2Cl_2, −90 °C): 2 very broad resonances between δ 40 and 15. $^{31}P\{^1H\}$ NMR (CD_2Cl_2, 0 or 20 °C): 16.4 (s).

Crystallography. $C_{46}H_{50}P_3Ru(PF_6)$ (2): fw = 941.9, monoclinic, space group $P2_1/n$, a = 18.884 (3) Å, b = 18.612 (3) Å, c = 12.361 (1) Å, β = 90.40 (1)°, V_c = 4344.4 Å^3, t = 22 (2) °C, ρ_{obsd} = 1.42 (1) g cm^{-3}, ρ_{calcd} = 1.44 g cm^{-3}, Z = 4, μ(Cu Kα) = 49.1 cm^{-1}. Pale orange, diffraction-quality crystals exhibiting forms {110}, {1$\bar{1}$0}, and {10$\bar{1}$} were grown from dichloromethane/ether. The selected specimen crystal had dimensions 0.13 × 0.18 × 0.15 mm between bounding faces. Reflection intensities were recorded with a Picker FACS-1 diffractometer operating in the θ–2θ continuous-scan mode (Cu Kα radiation, graphite monochromator, scan velocity 2° min^{-1} 2θ, 2 × 10 s backgrounds at extremes, $h,k,\pm l$, $3 < 2\theta < 125°$, 7673 measured reflections including standards (10,0,0, 0,10,0, 008 at 100 reflection intervals), 5787 unique observed reflections ($I \geq 3\sigma$)). Reflection intensities were corrected for crystal degradation[20] (maximum 10%) and specimen absorption effects (maximum/minimum transmission 0.65/0.46)[21] and were reduced to $|F_o|$ and $\sigma(F_o)$ values in the usual manner. R_s for this data set was 0.021, and R_{int} ($=\sum|F_o - \langle F_o\rangle|/\sum|F_o|$; 205 reflection pairs) was 0.022. The structure was solved by conventional Patterson and Fourier synthesis techniques and was refined by full-matrix least-squares analysis with reflection weights $w = [\sigma^2(F_o) + 0.002F_o^2]^{-1}$. All hydrogen atoms were visible in difference maps and, except for the phenyl hydrogens (located by calculation; C–H = 0.95 Å, $B_H = 1.1B_C$), were refined in the usual way (x, y, z, B). Anisotropic thermal parameters were specified for all non-hydrogen atoms, and in the final stages of refinement a variable extinction parameter[22] was also included in the scattering model. At convergence (maximum Δ/σ = 0.31) R = 0.042, R_w = 0.053, and S = 1.74. Electron density excursions in a final difference map did not exceed ±0.4 e Å^{-3}, and the terminal value of the secondary extinction parameter was [5.6 (4)] × 10^{-5}.

$C_{36}H_{50}P_3Ru(PF_6)$ (3): fw = 821.8, monoclinic, space group $C2/c$, a = 21.220 (8) Å, b = 23.412 (10) Å, c = 18.580 (7) Å, β = 126.05 (1)°, V_{calcd} = 7463.0 Å^3, t = 21 (2) °C, ρ_{calcd} = 1.46 g cm^{-3}, Z = 8, μ(Mo Kα) = 6.41 cm^{-1}; specimen crystal bounding forms/dimensions {110}/0.09, {1$\bar{1}$0}/0.10, {10$\bar{1}$}/0.28 mm; Picker FACS-1 diffractometer (Mo Kα radiation, graphite monochromator, 2° min^{-1} 2θ, 2 × 10 s backgrounds, $h,k,\pm l$, $3 < 2\theta < 60°$, 8894 measured reflections including standards (600, 0,$\bar{1}$0,0, 0,0,$\bar{1}$0), 5832 unique observed reflections ($I \geq 3\sigma$), degradation <0.5%, absorption correction applied (maximum/minimum transmission 0.96/0.93), R_s = 0.031, R_{int}(207 pairs) = 0.016). Systematic absences are consistent with either of the space groups Cc and $C2/c$, the centrosymmetric alternative, or a very close approximation thereof (vide infra), being confirmed by the structure solution and refinement (both as for **2**). No hydrogen atoms could be located with certainty by difference Fourier synthesis, even after extensive (anisotropic) refinement of all non-hydrogen atom parameters. Use of a low-temperature (130 K) but slightly less precise data set (5840 reflections, R_s = 0.044, R_{int} = 0.023) yielded an identical result; accordingly, only phenyl hydrogen atoms (positioned by calculation) were included in the final scattering model. Convergence parameters (maximum Δ/σ = 0.34) for the 21 °C data set were R = 0.053, R_w = 0.076, S = 1.99, and $-0.8 < \Delta\rho < 1.1$ e Å^{-3}. At 130 K the packing arrangement has less than full $C2/c$ symmetry. The structure factor agreement (in $C2/c$) is only marginally less good than that obtained at room temperature (R(130 K) = 0.059, R_w(130 K) = 0.079), but a difference map shows each atom site to be accompanied by a residual peak (ca. 15 e Å^{-3} for Ru, 5 e Å^{-3} for P, 1–2 e Å^{-3} for F, C) at a distance of ca. 0.05–0.15 Å. The "less than $C2/c$" symmetry may be due to the occurrence of chemically distinct cations in which the proton is attached either to C(11) or C(22), although other explanations are possible. There is no evidence or indication of a phase change, and the room-temperature structure almost certainly represents a symmetrized average over two crystallographically independent cations which may, or may not, be chemically distinct. Quoted cell dimensions are derived, in each instance, from least-squares analyses of setting angles for 12 carefully centered reflections ($43 < 2\theta < 60°$, **2**; $25 < 2\theta < 37°$, **3**). Atomic scattering factors with dispersion corrections for all non-H atoms were taken from ref 23. Final atomic coordinates (if refined) are listed, together with estimated standard errors, in Tables III and IV. Listings of observed and calculated structure factor amplitudes and of anisotropic thermal parameters for the non-hydrogen atoms have been included in the supplementary material. Computations were performed with ANUCRYS programs;[24] the figures were drawn with ORTEP.[25]

Results

Preparation of Precursors. We initially made a series of bis(nitrato)(η^6-hexamethylbenzene)ruthenium(II) complexes as shown in Scheme II. Treatment of $[RuCl_2(\eta^6\text{-}C_6Me_6)]_2$ with silver nitrate in acetone gives the orange complex $Ru(ONO_2)_2(\eta^6\text{-}C_6Me_6)$, which is monomeric in dichloromethane. Its molecular weight in nitromethane, however, is about half the formula weight and in this solvent the compound is a 1:1 electrolyte. The structure in the solid state is probably similar to that of Rh-

(20) Churchill, M. R.; Kalra, K. I. *Inorg. Chem.* **1974**, *13*, 1427.
(21) DeMeulenaer, J.; Tompa, H. *Acta Crystallogr.* **1965**, *19*, 104. Alcock, N. W. *Acta Crystallogr., Sect. A* **1969**, *25*, 518.
(22) Zachariasen, W. H. *Acta Crystallogr.* **1963**, *16*, 1139.
(23) *International Tables for X-ray Crystallography*; Kynoch Press: Birmingham, England, 1974; Vol. IV, pp 99, 149.
(24) McLaughlin, G. M.; Taylor, D.; Whimp, P. O. The ANUCRYS Structure Determination Package; Research School of Chemistry, The Australian National University: Canberra, Australia, 1977.
(25) Johnson, C. K. ORTEP II, Report ORNL-5138; Oak Ridge National Laboratory: Oak Ridge, TN, 1976.

Table III. Atomic Coordinates[a] and Equivalent Isotropic Thermal Parameters for $[Ru(C_{12}H_{17})(Ph_2PCH{=}CHPPh_2)(PMe_2Ph)]PF_6$ (2)

atom	x/a	y/b	z/c	B_{eq},[b] Å^2	atom	x/a	y/b	z/c	B_{eq},[b] Å^2
Ru	0.8616 (1)	0.2046 (1)	0.0594 (1)	2.7	C(312)	0.9377 (3)	0.1792 (3)	0.3675 (4)	4.7
P(1)	0.9328 (1)	0.3013 (1)	0.1015 (1)	3.5	C(313)	0.9720 (4)	0.2046 (3)	0.4592 (4)	6.3
P(2)	0.9263 (1)	0.1612 (1)	−0.0863 (1)	2.9	C(314)	1.0438 (5)	0.2110 (3)	0.4626 (5)	7.3
P(3)	0.9307 (1)	0.1288 (1)	0.1566 (1)	2.9	C(315)	1.0836 (3)	0.1932 (3)	0.3730 (5)	6.6
P(4)	0.2381 (1)	0.2133 (1)	0.0480 (1)	5.5	C(316)	1.0499 (3)	0.1677 (3)	0.2794 (4)	4.6
F(1)	0.3016 (3)	0.2631 (3)	0.0505 (6)	16.0	C(321)	0.8970 (2)	0.0429 (2)	0.2078 (4)	3.8
F(2)	0.2791 (3)	0.1456 (3)	0.0304 (6)	16.8	C(11)–C(1)–C(2)	116.4 (4)	117.1 (4)	C(2)–C(22)–H(22B)	120 (3)
F(3)	0.1707 (3)	0.1656 (3)	0.0501 (4)	13.5	C(322)	0.8458 (3)	0.0059 (3)	0.1517 (4)	4.6
F(4)	0.1938 (3)	0.2821 (3)	0.0702 (6)	15.7	C(323)	0.8239 (3)	−0.0622 (3)	0.1864 (5)	5.8
F(5)	0.2253 (4)	0.2216 (3)	−0.0723 (3)	14.5	C(324)	0.8523 (4)	−0.0918 (3)	0.2759 (6)	7.1
F(6)	0.2466 (5)	0.2021 (3)	0.1705 (4)	17.4	C(325)	0.9028 (4)	−0.0561 (3)	0.3322 (6)	8.0
C(111)	0.9054 (3)	0.3813 (2)	0.0263 (4)	4.5	C(326)	0.9253 (3)	0.0101 (3)	0.2983 (5)	6.2
C(112)	0.8428 (3)	0.4166 (3)	0.0526 (4)	5.8	C(1)	0.7429 (2)	0.1867 (2)	0.0058 (3)	3.5
C(113)	0.8222 (5)	0.4776 (3)	−0.0021 (6)	8.2	C(2)	0.7474 (2)	0.1800 (2)	0.1219 (3)	3.6
C(114)	0.8629 (6)	0.5045 (4)	−0.0848 (7)	9.7	C(3)	0.7191 (2)	0.1175 (3)	0.1732 (4)	4.4
C(115)	0.9232 (6)	0.4704 (4)	−0.1120 (6)	9.2	C(4)	0.6825 (2)	0.0685 (3)	0.1102 (5)	5.0
C(116)	0.9456 (4)	0.4084 (3)	−0.0577 (5)	6.6	C(5)	0.6773 (3)	0.0764 (3)	−0.0036 (4)	4.9
C(121)	1.0277 (3)	0.2987 (3)	0.0814 (5)	4.8	C(6)	0.7079 (2)	0.1336 (3)	−0.0558 (4)	4.1
C(131)	0.9291 (4)	0.3363 (3)	0.2390 (5)	4.9	C(11)	0.7644 (3)	0.2576 (3)	−0.0407 (4)	4.0
C(201)	0.9997 (2)	0.1094 (2)	−0.0328 (3)	3.5	C(22)	0.7846 (3)	0.2372 (3)	0.1785 (4)	4.1
C(211)	0.9663 (2)	0.2276 (2)	−0.1750 (3)	3.7	C(33)	0.7272 (4)	0.1098 (5)	0.2944 (5)	6.5
C(212)	1.0388 (3)	0.2353 (3)	−0.1856 (4)	4.9	C(44)	0.6466 (5)	0.0051 (5)	0.1643 (8)	7.8
C(213)	1.0660 (3)	0.2871 (4)	−0.2547 (5)	6.7	C(55)	0.6369 (5)	0.0195 (5)	−0.0696 (10)	8.0
C(214)	1.0211 (4)	0.3307 (3)	−0.3136 (5)	7.1	C(66)	0.7021 (5)	0.1417 (4)	−0.1765 (5)	5.7
C(215)	0.9502 (4)	0.3234 (3)	−0.3050 (4)	6.3	H(66A)	0.714 (4)	0.099 (4)	−0.229 (6)	10.8 (21)
C(216)	0.9217 (3)	0.2717 (3)	−0.2361 (4)	4.7	H(66B)	0.667 (5)	0.167 (5)	−0.199 (7)	12.7 (29)
C(221)	0.8911 (2)	0.0960 (2)	−0.1855 (3)	3.5	H(66C)	0.732 (4)	0.157 (4)	−0.207 (5)	6.8 (22)
C(222)	0.8530 (3)	0.0381 (3)	−0.1491 (4)	4.9	H(121A)	1.042 (3)	0.287 (2)	0.007 (4)	4.4 (11)
C(223)	0.8268 (3)	−0.0141 (3)	−0.2180 (5)	5.7	H(121B)	1.040 (4)	0.339 (4)	0.091 (6)	10.3 (23)
C(224)	0.8383 (4)	−0.0080 (3)	−0.3249 (5)	6.5	H(121C)	1.046 (3)	0.267 (3)	0.136 (4)	5.7 (13)
C(225)	0.8743 (5)	0.0496 (4)	−0.3635 (5)	9.7	H(122A)	0.951 (3)	0.374 (3)	0.239 (4)	4.2 (11)
C(226)	0.9012 (4)	0.1016 (3)	−0.2935 (4)	7.9	H(122B)	0.886 (3)	0.339 (3)	0.261 (5)	7.6 (19)
C(301)	1.0012 (2)	0.0953 (2)	0.0706 (4)	3.6	H(122C)	0.942 (3)	0.303 (3)	0.305 (4)	6.1 (13)
C(311)	0.9773 (2)	0.1610 (2)	0.2769 (3)	3.5	H(201)	1.033 (2)	0.095 (2)	−0.077 (3)	2.9 (8)
					H(301)	1.032 (2)	0.066 (2)	0.101 (3)	3.5 (9)

[a] Phenyl hydrogen atom coordinates (not listed) located by calculation (C–H = 0.95 Å) and not refined. [b] $B_{eq} = {}^1/_3\sum_i\sum_j\beta_{ij}a^*_i a^*_j \mathbf{a}_i\cdot\mathbf{a}_j$. [c] Actual values for hydrogen atoms.

$(ONO_2)_2(\eta^5\text{-}C_5Me_5)$, which has one bidentate and one monodentate nitrato group;[26] in nitromethane, one of the anions must ionize. The complex $[Ru(ONO_2)(\eta^6\text{-}C_6Me_6)(PMe_2Ph)_2]NO_3$ formed by treatment of $Ru(ONO_2)_2(\eta^6\text{-}C_6Me_6)$ with dimethylphenylphosphine is a yellow, air-sensitive solid whose ^1H NMR spectrum contains two multiplets (virtual triplets or filled-in doublets) for the methyl groups of the PMe_2Ph ligands. Thus, the methyl groups of each PMe_2Ph ligand are inequivalent and there is no plane of symmetry along the Ru-P axis. The IR spectra of this and the other, similarly prepared P-donor complexes show bands typical of monodentate nitrate at ca 1270 cm^{-1} and 1000 cm^{-1}.[26]

Scheme II

$$[RuCl_2(\eta^6\text{-}C_6Me_6)]_2 \xrightarrow{2AgNO_3} Ru(ONO_2)_2(\eta^6\text{-}C_6Me_6) \xrightarrow[\text{acetone}]{2L} [Ru(ONO_2)(\eta^6\text{-}C_6Me_6)L_2]NO_3$$

L = PPh_3, PMe_2Ph, $P(OMe)_3$, $P(OCH_2)_3CMe$, $\frac{1}{2}Ph_2PCH_2CH_2PPh_2$

Although $Ru(ONO_2)_2(\eta^6\text{-arene})$ complexes containing benzene, *o*-xylene, mesitylene, and durene can be prepared similarly to the hexamethylbenzene analogue, the coordinated arene in these complexes is readily displaced by P-donor ligands and complexes of the type $[Ru(ONO_2)(\eta^6\text{-arene})L_2]NO_3$ could not be made. We therefore turned to the cationic trifluoroacetato complexes $[Ru(O_2CCF_3)(\eta^6\text{-arene})L_2]^+$ (Scheme III). Treatment of $[RuCl_2(\eta^6\text{-arene})]_2$ (arene = C_6Me_6, 1,2,4,5-$C_6H_2Me_4$, 1,2-$C_6H_4Me_2$) with silver acetate gives the monomeric bis(acetato) complexes $Ru(O_2CMe)_2(\eta^6\text{-arene})$, which react with trifluoroacetic acid to give the corresponding bis(trifluoroacetato) complexes $Ru(O_2CCF_3)_2(\eta^6\text{-arene})$.[27] These need not be isolated in a pure state; direct reaction with the P-donor ligand (ca. 3 equiv) in methanol in the presence of NH_4PF_6 gives $[Ru(O_2CCF_3)(\eta^6\text{-arene})L_2]PF_6$ in 70–80% yield based on $[RuCl_2(\eta^6\text{-arene})]_2$.

Scheme III

$$[RuCl_2(\eta^6\text{-arene})]_2 \xrightarrow[\text{1. } CF_3CO_2H]{2AgO_2CMe} Ru(O_2CMe)_2(\eta^6\text{-arene}) \xrightarrow[\text{3. } NH_4PF_6]{\text{2. L (ca. 3 equiv)}} [Ru(O_2CCF_3)(\eta^6\text{-arene})L_2]PF_6$$

arene = C_6Me_6, L = $PMePh_2$, $\frac{1}{2}\{(Z)\text{-}Ph_2PCH{=}CHPPh_2\}$; arene = 1,2,4,5-$C_6H_2Me_4$, L = PMe_2Ph, $PMePh_2$, $\frac{1}{2}\{(Z)\text{-}Ph_2PCH{=}CHPPh_2\}$; arene = 1,2-$C_6H_4Me_2$, L = PMe_2Ph, $PMePh_2$

Occasionally, the alternative route outlined in Scheme IV was employed. Treatment of $[RuCl_2(\eta^6\text{-arene})]_2$ (arene = 1,2,4,5-$C_6H_2Me_4$, 1,2-$C_6H_4Me_2$, C_6H_6) with tetramethyltin in acetonitrile gives in situ the neutral monomethyl derivatives $RuClMe(\eta^6\text{-arene})(NCMe)$,[28] which

(26) Hursthouse, M. B.; Abdul Malik, K. M.; Mingos, D. M. P.; Willoughby, S. D. *J. Organomet. Chem.* **1980**, *192*, 235.

(27) Tocher, D. A.; Gould, R. O.; Stephenson, T. A.; Bennett, M. A.; Ennett, J. P.; Matheson, T. W.; Sawyer, L.; Shah, V. K. *J. Chem. Soc., Dalton Trans.* **1983**, 1571.

(28) Zelonka, R. A.; Baird, M. C. *J. Organomet. Chem.* **1972**, *44*, 383.

react with PMe_2Ph to give $RuClMe(\eta^6\text{-arene})(PMe_2Ph)$. Treatment of these complexes with another 1 equiv of PMe_2Ph in methanol in the presence of NH_4PF_6 gives the cationic methyl complexes $[RuMe(\eta^6\text{-arene})(PMe_2Ph)_2]PF_6$.[29] The Ru–Me bond is readily cleaved by trifluoroacetic acid[30] to give the required trifluoroacetato complexes $[Ru(O_2CCF_3)(\eta^6\text{-arene})(PMe_2Ph)_2]PF_6$. Neither method proved satisfactory for the preparation of cationic η^6-*o*-xylene trifluoroacetato complexes containing trimethyl phosphite or 1,2-bis(diphenylphosphino)ethane, because the arene was easily displaced by the P-donor ligands.

Scheme IV

$$[RuCl_2(\eta^6\text{-arene})]_2 \xrightarrow[2.\ L]{1.\ Me_4Sn/MeCN} RuClMe(\eta^6\text{-arene})L \xrightarrow[2.\ NH_4PF_6]{1.\ L/MeOH} [RuMe(\eta^6\text{-arene})L_2]PF_6 \xrightarrow{CF_3CO_2H} [Ru(O_2CCF_3)(\eta^6\text{-arene})L_2]PF_6$$

arene = 1,2,4,5-$C_6H_2Me_4$, 1,2-$C_6H_4Me_2$, C_6H_6

The cationic trifluoroacetato complexes have been characterized by elemental analysis and by their NMR (^1H, ^{31}P) spectra (see Experimental Section), which are generally unexceptional. Unexpectedly, however, the spectra of $[Ru(O_2CCF_3)(\eta^6\text{-}o\text{-}C_6H_4Me_2)(PMePh_2)_2]PF_6$ show the presence in solution of two isomers. These may be conformers arising from restricted rotation about the Ru–P, P–C(phenyl), or Ru–arene bonds as a consequence of the crowded environment of the metal atom, but it is surprising that the presumably more crowded analogues containing hexamethylbenzene or durene do not behave similarly.

***o*-Xylylene Complexes.** Treatment of THF suspensions of the salts $[Ru(ONO_2)(\eta^6\text{-arene})L_2]NO_3$ or $[Ru(O_2CCF_3)(\eta^6\text{-arene})L_2]PF_6$ containing hexamethylbenzene, durene, or *o*-xylene with potassium *tert*-butoxide in the presence of 1 mol equiv of a tertiary phosphine (L′) gives the (*o*-xylylene)ruthenium(0) complexes $Ru(o\text{-xylylene})L_2L'$ as colorless or pale yellow solids of moderate air stability (eq 2). Yields of isolated products are generally

$$[RuX\{\eta^6\text{-}C_6R_2R'_2(CH_3)_2\}L_2]Y + L' \rightarrow Ru\{\eta^4\text{-}(CH_2)_2C_6R_2R'_2\}L_2L' + HX + HY \quad (2)$$

R = R′ = Me; X = Y = ONO_2; L = L′ = $P(OMe)_3$, $P(OCH_2)_3CMe$

R = R′ = Me; X = Y = ONO_2; $L_2 = Ph_2PCH_2CH_2PPh_2$; L′ = PMe_2Ph

R = R′ = Me; X = O_2CCF_3; Y = PF_6; L = L′ = PMe_2Ph, $PMePh_2$

R = R′ = Me; X = O_2CCF_3; Y = PF_6; L_2 = (*Z*)-$Ph_2PCH{=}CHPPh_2$; L′ = PMe_2Ph

R = R′ = Me; X = O_2CCF_3; Y = PF_6; L = L′ = PMe_2Ph

R = H; R′ = Me; X = O_2CCF_3; Y = PF_6; L = L′ = PMe_2Ph, $PMePh_2$

R = R′ = H; X = O_2CCF_3; Y = PF_6; L = L′ = PMe_2Ph

in the range 20–80%, being highest for C_6Me_6 and lowest for *o*-$C_6H_4Me_2$. The ^1H NMR spectra of the complexes show a characteristic pair of 2 H multiplets at δ ca. 0 and 2 due to the inner and outer protons H^1 and H^2, respectively, of the coordinated exocyclic double bond; these resonances appear as doublets (J ca. 4 Hz) in the $^1H\{^{31}P\}$ NMR spectra. A similar pattern has been observed in other exodentate *o*-xylylene complexes; e.g., η^4-$C_6H_4(CH_2)_2Fe(CO)_3$ has δ 0.03 (d, J_{12} = 3.2 Hz, H^1) and 2.33 (d, H^2).[8] In the $^{13}C\{^1H\}$ NMR spectra the resonance due to the outer carbon atoms of the exocyclic diene is also highly shielded, appearing as a triplet in the region δ 20–30 owing to coupling with two ^{31}P nuclei, and the signal due to the inner carbon atoms is in the region of δ 100. As expected, the *o*-xylylene methyl groups in the complexes derived from hexamethylbenzene are inequivalent and give rise to two 6 H singlets in the region δ 2.0–2.5, whereas those derived from durene give just one 3 H singlet in the same region.

The X-ray structure of $Ru\{\eta^4\text{-}o\text{-}(CH_2)_2C_6H_4\}(PMe_2Ph)_3$ shows the coordination geometry to be very similar to that

Table IV. Atomic Coordinates[a] and Equivalent Isotropic Thermal Parameters[b] for $[Ru(C_{12}H_{17})(PMe_2Ph)_3]PF_6$ (3)

atom	*x/a*	*y/b*	*z/c*	B_{eq}, Å^2
Ru	0.3268 (1)	0.6492 (1)	0.3703 (1)	2.3
P(1)	0.3177 (1)	0.5526 (1)	0.3590 (1)	3.4
P(2)	0.4554 (1)	0.6531 (1)	0.4250 (1)	2.9
P(3)	0.2847 (1)	0.6690 (1)	0.2248 (1)	3.5
C(1)	0.3234 (3)	0.7097 (2)	0.4729 (4)	3.0
C(2)	0.2562 (3)	0.7189 (2)	0.3878 (4)	3.4
C(3)	0.2338 (4)	0.7754 (3)	0.3526 (5)	4.7
C(4)	0.2802 (5)	0.8199 (3)	0.4046 (6)	6.1
C(5)	0.3460 (5)	0.8116 (3)	0.4908 (6)	5.3
C(6)	0.3677 (4)	0.7571 (3)	0.5265 (5)	4.3
C(11)	0.3413 (4)	0.6503 (2)	0.5049 (5)	4.2
C(22)	0.2083 (4)	0.6674 (3)	0.3419 (5)	5.8
C(33)	0.1612 (5)	0.7854 (4)	0.2621 (6)	8.7
C(44)	0.2577 (8)	0.8818 (3)	0.3664 (8)	10.3
C(55)	0.3969 (7)	0.8624 (4)	0.5471 (8)	9.7
C(66)	0.4354 (5)	0.7478 (4)	0.6213 (5)	7.0
C(111)	0.2401 (3)	0.5266 (2)	0.3655 (4)	3.6
C(112)	0.2490 (4)	0.5150 (2)	0.4431 (5)	4.5
C(113)	0.1884 (5)	0.4953 (3)	0.4459 (6)	5.6
C(114)	0.1196 (5)	0.4879 (3)	0.3705 (7)	7.1
C(115)	0.1084 (4)	0.4995 (4)	0.2908 (7)	8.3
C(116)	0.1682 (4)	0.5188 (3)	0.2880 (5)	5.5
C(121)	0.3982 (4)	0.5114 (3)	0.4531 (6)	6.5
C(131)	0.3046 (5)	0.5132 (3)	0.2639 (6)	6.0
C(211)	0.4936 (3)	0.7201 (2)	0.4155 (3)	3.0
C(212)	0.5280 (4)	0.7257 (3)	0.3687 (4)	4.4
C(213)	0.5544 (4)	0.7775 (3)	0.3618 (5)	5.5
C(214)	0.5491 (4)	0.8239 (3)	0.4016 (5)	5.3
C(215)	0.5164 (4)	0.8203 (2)	0.4489 (4)	4.5
C(216)	0.4892 (3)	0.7684 (2)	0.4542 (4)	3.7
C(221)	0.5208 (3)	0.6417 (3)	0.5457 (4)	4.2
C(231)	0.4944 (4)	0.6006 (2)	0.3852 (5)	4.4
C(311)	0.2777 (4)	0.7431 (3)	0.1911 (4)	4.0
C(312)	0.2295 (5)	0.7604 (3)	0.1031 (5)	5.5
C(313)	0.2303 (5)	0.8166 (4)	0.0803 (5)	6.9
C(314)	0.2751 (5)	0.8560 (3)	0.1419 (6)	6.5
C(315)	0.3235 (4)	0.8399 (3)	0.2304 (6)	5.5
C(316)	0.3233 (4)	0.7841 (3)	0.2534 (4)	4.4
C(321)	0.3362 (5)	0.6407 (3)	0.1780 (5)	5.3
C(331)	0.1878 (4)	0.6418 (3)	0.1436 (4)	5.8
P(4)	0.0	0.9574 (1)	0.25	4.6
F(1)	0.0195 (4)	0.9594 (2)	0.1793 (4)	10.0
F(2)	0.0803 (4)	0.9471 (6)	0.3219 (5)	12.9
F(3)	0.0	0.8936 (4)	0.25	17.7
F(4)	0.0	1.0186 (3)	0.25	23.2
P(5)	0.5	0.0	0.0	4.9
F(5)	0.5135 (3)	0.0465 (2)	0.0695 (3)	9.2
F(6)	0.5208 (6)	−0.0451 (2)	0.0701 (4)	15.6
F(7)	0.5822 (4)	0.0048 (4)	0.0330 (6)	18.9

[a] Phenyl hydrogen atoms only in scattering model: located by calculation. [b] $B_{eq} = {}^1/_3\sum_i\sum_j\beta_{ij}a^*_i a^*_j \mathbf{a}_i\cdot\mathbf{a}_j$.

(29) Compounds of this type have also been synthesized by treatment of $Ru(\eta^6\text{-arene})(PR_3)_2$ with CH_3I and subsequent reaction with NH_4PF_6: Werner, R.; Werner, H. *Chem. Ber.* **1982**, *115*, 3781.

(30) Werner, H.; Kletzin, H. *J. Organomet. Chem.* **1982**, *228*, 289.

Scheme V

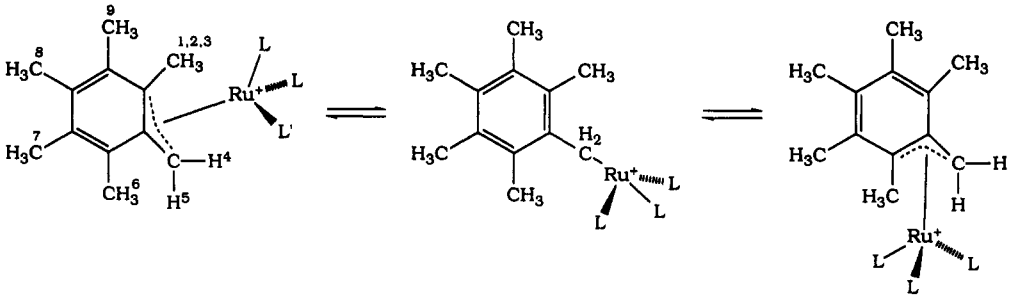

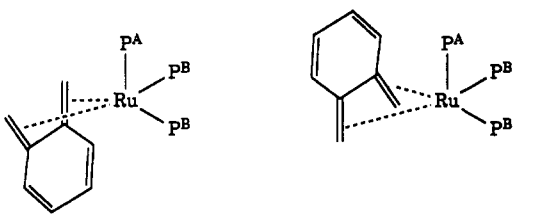

VI VII

Figure 2. Limiting conformations of Ru(*o*-xylylene)$(PR_3)_3$ complexes.

of a (1,3-diene)iron tricarbonyl complex, i.e. distorted square pyramidal with the diene fragment occupying two basal sites.[10] As shown in Figure 2, there are two possible limiting conformations, VI and VII; in the solid state the sterically much more favorable conformation VI, in which the axial phosphorus atom is exo to the six-membered ring, is adopted. The ^1H and ^{31}P NMR spectra suggest that this structure is retained in solution. For example, the $^1H\{^{31}P\}$ NMR spectrum of Ru{η^4-*exo*-$(CH_2)_2C_6H_4$}$\{P(OMe)_3\}_3$ shows two singlets at δ 3.65 and 3.25 in a 1:2 ratio due to the methyl groups of the inequivalent $P(OMe)_3$ ligands. Correspondingly, the $^{31}P\{^1H\}$ NMR spectrum shows a triplet at δ 175.7 due to the apical phosphorus atom P_A and a doublet at δ 154.4 due to the basal phosphorus atoms P_B ($^2J_{PP}$ = 34 Hz). The $^{31}P\{^1H\}$ NMR spectra of the other complexes are similar, although, as noted by Cole-Hamilton et al.,[10] the P–P couplings are smaller than those of the trimethyl phosphite complex. In the ^1H NMR spectra of the dimethylphenylphosphine complexes, the methyl resonances of the basal PMe_2Ph groups appear as a pair of filled-in doublets (virtual triplets), because there is no plane of symmetry along the Ru–P_B axis.

Protonation. Treatment of solutions in ether of the tetramethyl-*o*-xylylene complexes [Ru{η^4-*exo*-$(CH_2)_2C_6Me_4$}(L-L)(PMe_2Ph)]$^+$ (L-L = $Ph_2PCH_2CH_2PPh_2$, (*Z*)-$Ph_2PCH{=}CHPPh_2$) or Ru{η^4-*exo*-$(CH_2)_2C_6Me_4$}-$(PMe_2Ph)_3$ with 60% aqueous HPF_6 precipitates the PF_6 salts of the (tetramethyl-η^3-benzyl)ruthenium(II) cations [Ru{η^3-$(HCH_2)(CH_2)C_6Me_4$}(L-L)L′]$^+$ (L-L = $Ph_2PCH_2CH_2PPh_2$, L′ = PMe_2Ph (1); L-L = (*Z*)-$Ph_2PCH{=}CHPPh_2$, L′ = PMe_2Ph (2) and Ru{η^3-$(HCH_2)(CH_2)C_6Me_4$}$(PMe_2Ph)_3$ (3)) (Chart I). The fluxional behavior of these salts suggests that the proton adds to one of the terminal diene carbon atoms to form a three-center, two-electron (agostic) bond with the electron-deficient, 16e ruthenium atom;[31] this is confirmed by the X-ray structural analysis of complexes 2 and 3 discussed below.

The variation of the ^1H NMR spectrum of 1 with temperature was described in a preliminary communication.[16] In an attempt to simplify the spectra, we prepared and

Chart I

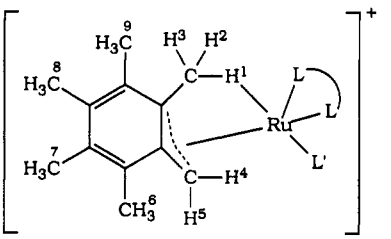

L-L = $Ph_2PCH_2CH_2PPh_2$, L′ = PMe_2Ph (**1**)
L-L = *Z*-$Ph_2PCH{=}CHPPh_2$, L′ = PMe_2Ph (**2**) or $P(CD_3)_2Ph$ (**2a**)

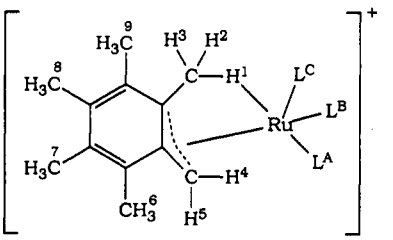

L = PMe_2Ph (**3**) or $P(CD_3)_2Ph$ (**3a**)

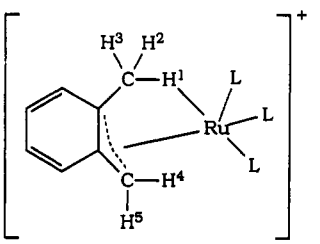

L = PMe_2Ph (**4**)

studied the $P(CD_3)_2(C_6H_5)$ analogues of 2 and 3 (**2a** and **3a**). The ^1H NMR spectrum of **2a** at −90 °C (Figure 3) shows a broad, three-proton resonance at δ −2.20 ($w_{1/2}$ = 30 Hz) due to the agostic methyl protons ($H^{1,2,3}$), which sharpens when the solution is warmed to −60 °C ($w_{1/2}$ = 18 Hz) and appears as a doublet (J_{PH} ca. 6 Hz). The protons $H^{1,2,3}$ evidently undergo reversible exchange, either by reversible Ru–H bond breaking or by "in-place" rotation,[32] but this exchange could not be frozen out. The resonances due to the protons of the η^3-benzyl group occur to a doublet at δ 0.78 (J_{HH} = 5.9 Hz) assigned to H^4 and a doublet of doublets at δ 3.24 (J_{PH} = 1.4 Hz) due to H^5, and the protons of the inequivalent methyl groups $H^{6,7,8,9}$ give rise to four singlets at δ 1.61, 1.74, 1.97, and 2.19. Between −30 and 0 °C the resonances due to $H^{1,2,3}$, H^4, and H^5 broaden and at 25 °C have almost disappeared into the base line. In the same temperature range, the methyl

(31) Review: Brookhart, M.; Green, M. L. H.; Wong, L.-L. *Prog. Inorg. Chem.* **1988**, *36*, 1.

(32) Green, M. L. H.; Wong, L.-L. *J. Chem. Soc., Chem. Commun.* **1988**, 677.

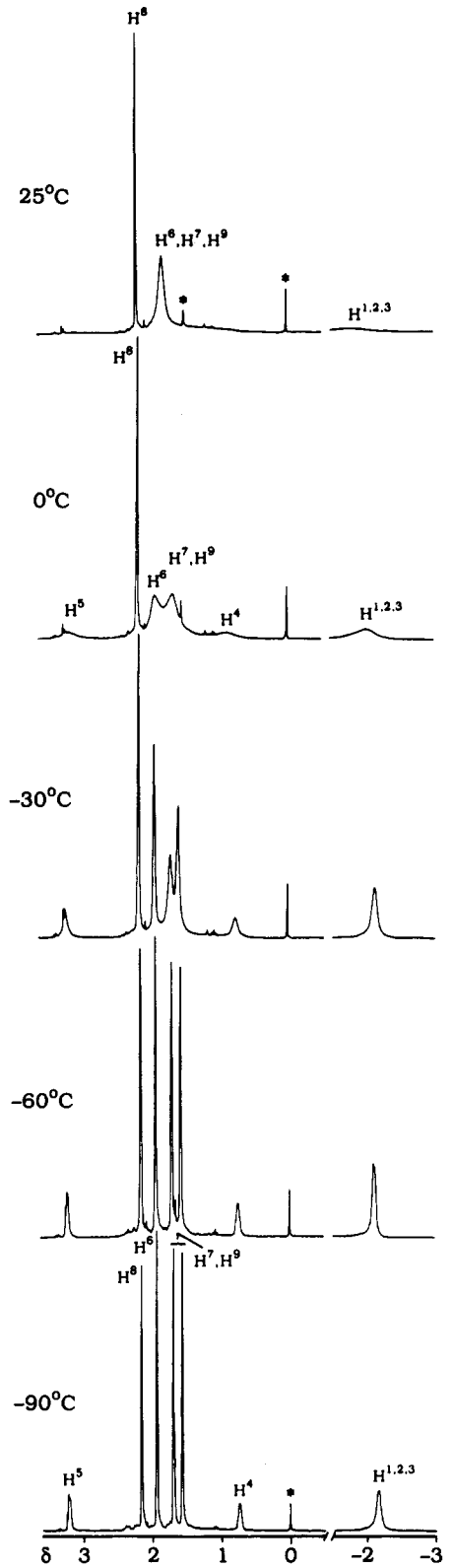

Figure 3. ^1H NMR spectra at 270 MHz of $[Ru\{\eta^3\text{-}(HCH_2)(CH_2)C_6Me_4\}\{(Z)\text{-}Ph_2PCH{=}CHPPh_2\}\{P(CD_3)_2Ph\}]PF_6$ (**2a**) in CD_2Cl_2 between −90 and +25 °C. Peaks marked with an asterisk are due to impurities or artifacts.

resonances at δ 1.61 and 1.74 collapse and coalesce, while the resonance at δ 1.97 broadens; the resonance at δ 2.19, however, remains sharp. At 0 °C only two broad resonances and a sharp singlet at δ 2.19 are observed.

These changes can be accounted for by assuming that there is a reversible change from η^3 to η^1 in the bonding mode of the benzyl fragment (Scheme V), similar to that established as the most likely mode of rearrangement for η^3-benzyl complexes of the type $M(\eta^5\text{-}C_5H_5)(\eta^3\text{-}CH_2Ar)(CO)_2$ (M = Mo, W)[33] and suggested for (η^3-benzyl)palladium(II) complexes such as $[PdCl(\eta^3\text{-}CH_2C_6H_3Me_2\text{-}3,4)]_2$ in $CDCl_3$[34] and $[Pd(\eta^3\text{-}CH_2C_6H_4)(PEt_3)_2]^+$ in CD_3CN.[35] This process generates a time-averaged plane of symmetry along the Ru–CH_2 axis passing through CH_3[8], thus causing the benzylic protons H^4 and H^5 to become equivalent, provided that there is free rotation about the Ru–C bond. In addition, the pairs of methyl protons $H^{1,2,3}$ and H^6, and H^7 and H^9, will become separately equivalent, while H^8 is unaffected. Because the protons of the latter pair differ less in chemical shift than those of the former, they will coalesce at a lower temperature. On this basis, we assign the unchanged singlet at δ 2.19 to H^8, the singlet at δ 1.97 to H^6, and the pair at δ 1.74 and 1.61 to H^7 and H^9 (or H^9 and H^7). The P–Me groups in **2** are inequivalent because there is no plane of symmetry down the Ru–P axis, and as expected, the PMe_2Ph resonances in the ^1H NMR spectrum of **2** between −80 and −30 °C appear as a pair of doublets, at δ 0.61 (J_{PH} = 10 Hz) and δ 1.12 (J_{PH} = 8 Hz). Above −30 °C these resonances broaden and coalesce, as shown in Figure 4; they reappear at 30 °C as a sharp doublet at δ 0.90 (J_{PH} = 9 Hz). The P–Me groups are now apparently equivalent, because the $\eta^3 \rightleftarrows \eta^1$ interconversion generates a time-averaged symmetry plane down the Ru–P axis.

As the temperature of the solution is increased, the resonance due to $H^{1,2,3}$ collapses into the base line and at 40 °C a broad resonance appears at δ −0.20, which is assigned to the average of $H^{1,2,3}$ and H^6 (Figure 5). This sharpens on further heating and at 80 °C has a half-width of 15 Hz. The peak arising from the averaging of H^4 and H^5 could not be located with certainty, but its expected position (δ ca. 2.0) suggests that it may be masked by the singlet due to H^8 at δ ca. 2.1. In the temperature range 60–80 °C this singlet and that due to H^7, H^9 (average) at δ 1.80 begin to broaden and collapse, whereas the P–Me doublet remains sharp. This behavior is indicative of the onset of a third process in which the agostic C–H bonds are reversibly broken and re-formed via a diene–hydride intermediate (Scheme VI). In combination with the two processes already discussed, the highest energy process allow the complexed ruthenium fragment to migrate around the six-membered ring, thus leading finally to the equivalence of all 17 protons.

The coalescence temperature for the averaging of $H^{1,2,3}$ with H^6 is estimated to be 30 °C, and the rate of the $\eta^3 \rightleftarrows \eta^1$ interconversion at this temperature obtained from the standard equation $k = \pi\Delta\nu/2^{1/2}$ is 2433 s^{-1}, corresponding to a free energy of activation ($\Delta G^\ddagger$) of 13.0 kcal/mol. For the resonances due to H^7 and H^9 the coalescence temperature is about 0 °C, although this is more difficult to assess owing to the simultaneous broadening of the nearby singlet due to H^6; the corresponding rate is 77 s^{-1}, and the derived value of $\Delta G^\ddagger$ is 12.2 kcal/mol. Measurements of the line width of the resonance due to $H^{1,2,3}$ at −30 and 0 °C and application of the slow-exchange approximation $k = \pi(w_{1/2} - w^0_{1/2})$ give $\Delta G^\ddagger$ values of 12.0 and 12.6 kcal/mol, respectively, which are in reasonable agreement with the estimates derived from the coalescence temperatures.

In principle, it should also be possible to detect the $\eta^3 \rightleftarrows \eta^1$ interconversion of the benzyl group in **2** by examination of the variable-temperature $^{31}P\{^1H\}$ NMR spectrum,

(33) Cotton, F. A.; Marks, T. J. *J. Am. Chem. Soc.* **1969**, *91*, 1339.
(34) Roberts, J. S.; Klabunde, K. J. *J. Am. Chem. Soc.* **1977**, *99*, 2509.
(35) Becker, Y.; Stille, J. K. *J. Am. Chem. Soc.* **1978**, *100*, 845.

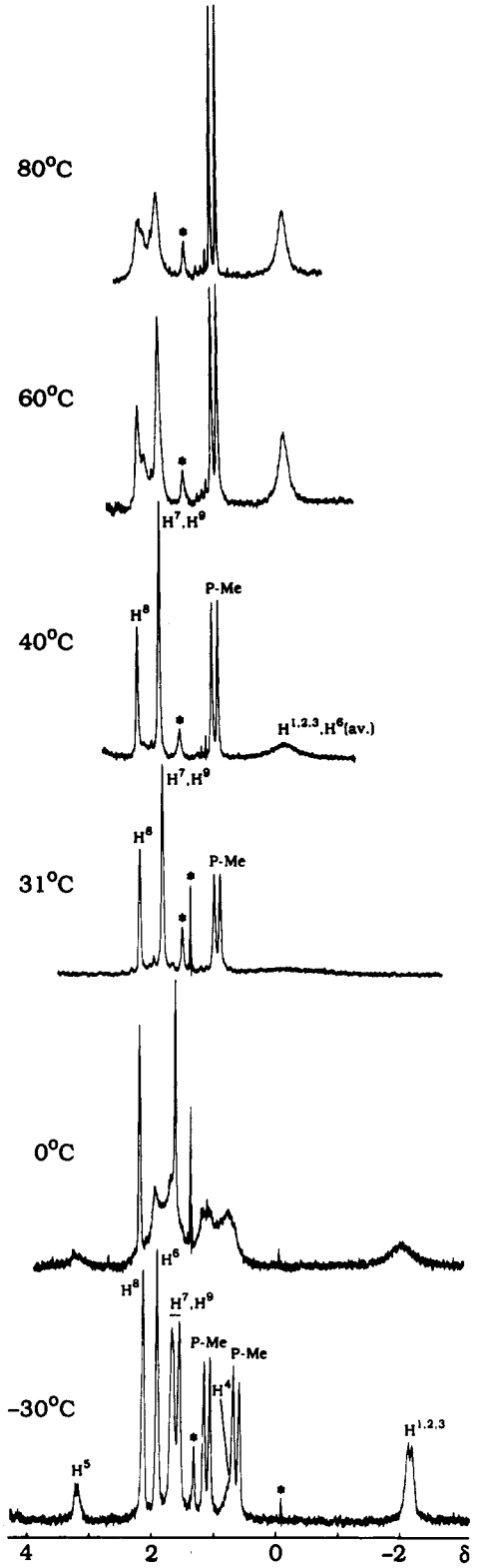

Figure 4. ^1H NMR spectra at 100 MHz of $[Ru\{\eta^3\text{-}(HCH_2)(CH_2)C_6Me_4\}\{(Z)\text{-}Ph_2PCH{=}CHPPh_2\}(PMe_2Ph)]PF_6$ (2) in 1,2-$C_2H_4Cl_2$ between -30 and +80 °C. Peaks marked with an asterisk are due to impurities or artifacts.

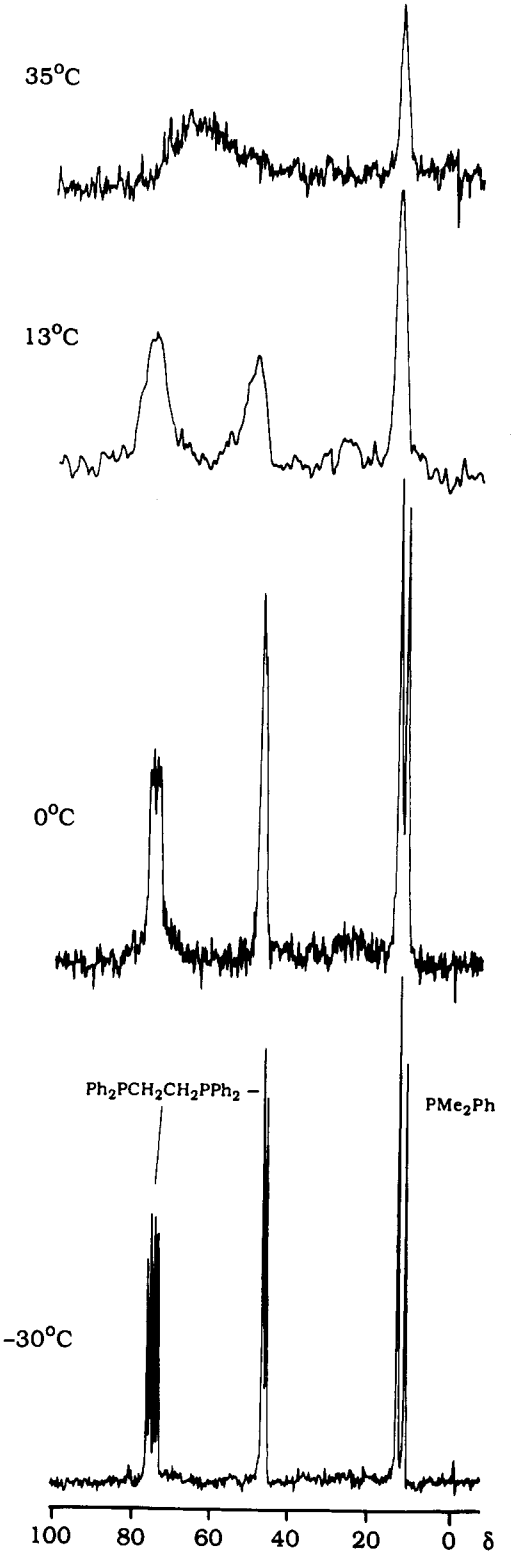

Figure 5. Variable temperature $^{31}P\{^1H\}$ NMR spectra at 24.3 MHz of $[Ru\{\eta^3\text{-}(HCH_2)(CH_2)C_6Me_4\}(Ph_2PCH_2CH_2PPh_2)(PMe_2Ph)]PF_6$ (1) in CH_2Cl_2. At 76 °C in 1,2-$C_2H_4Cl_2$ the two peaks evident at 35 °C sharpen further to a doublet at δ 66.6 and a triplet at δ 13.5, but peaks arising from decomposition also appear. The septet due to PF_6^- is not shown.

because the process should average the environments of the phosphorus atoms of the bidentate ligand. The $^{31}P\{^1H\}$ NMR spectrum of **2** at -55 °C contains, in addition to the septet due to PF_6^-, a pair of complex multiplets in a ratio of about 2:1. These change slightly in appearance as the temperature is raised to 20 °C, but the chemical shifts of the phosphorus atoms of (*Z*)-$Ph_2PCH{=}CHPPh_2$ in **2** are clearly too similar for any conclusions to be drawn. The $^{31}P\{^1H\}$ NMR spectrum of **1** is more informative (Figure 5). In the temperature range -60 to -30 °C it consists of three resonances of equal intensity at δ 77.6 (dd, J_{PP} = 43.9, 19.5 Hz), 49.1 (d, J_{PP} = 19.5 Hz), and δ 14.4 (d, J_{PP} = 43.9 Hz). As the temperature is raised, the first two signals broaden, collapse, and coalesce at about 30 °C, while the third signal also broadens. At 76 °C the spectrum consists

Scheme VI

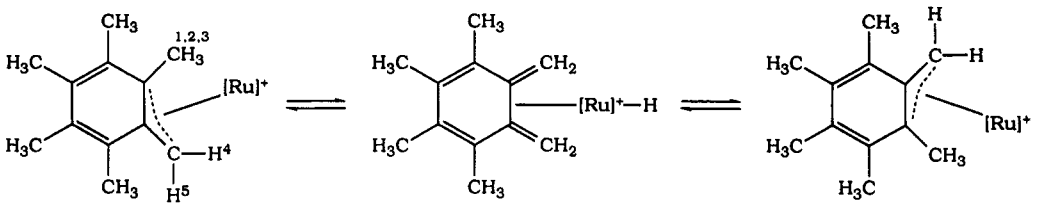

[Ru] = RuL_3

of a doublet at δ 66.6 due to the averaged ^{31}P environments of $Ph_2PCH_2CH_2PPh_2$ and a triplet at δ 13.5 (J ca. 19 Hz) due to PMe_2Ph, in addition to peaks arising from decomposition products. The rate of interconversion at the coalescence temperature is 1534 s^{-1}, corresponding to a free energy of activation $\Delta G^{\ddagger}$ of 13.3 kcal/mol, which agrees reasonably with the values obtained for **2** from the ^1H NMR spectra.

The variable-temperature ^1H NMR spectrum of **3a** suggests that this complex is similar to, but more fluxional than, **2a** (Figure 6). At −90 °C the spectrum consists of a broad resonance ($w_{1/2}$ ca. 170 Hz) at δ −2.5 assigned to $H^{1,2,3}$, broad peaks at δ ca. 0.6 and 2.7 due to H^4 and H^5, respectively, and partially overlapping singlets in the range δ 1.9–2.2 due to the methyl groups of the six-membered ring. At −60 °C all these peaks, except for a methyl singlet at δ 2.21, broaden and at −30 °C the peaks due to $H^{1,2,3}$, H^4, and H^5 collapse into the base line, while the methyl resonances consist of two sharp singlets in a 1:2 ratio at δ 2.26 (H^8) and δ 2.13 (H^7, H^9). At 0 °C a broad 6 H resonance appears at δ ca. 0.1 due to the averaging of $H^{1,2,3}$ with H^6, and broadening of both methyl resonances is evident; a singlet at δ ca. 1.6 may be due to the resonance of H^4, H^5 (average), but the presence of impurity peaks in the region of δ 1.8 makes unambiguous assignment impossible. In the ^1H NMR spectrum of **3** at −90 °C, the P–Me resonances appear as a triplet of relative intensity 1 at δ 1.11 (separation ca. 8 Hz) and a multiplet of relative intensity 2 centered at δ 1.31; these coalesce to a broad singlet at 0 °C.

It is clear from a comparison of the approximate coalescence temperatures for the exchange of $H^{1,2,3}$ with H^6 that the $\eta^3 \rightleftarrows \eta^1$ interconversion of the benzyl group occurs more easily in **3** than in **2**. For **3a**, the coalescence temperature is about −30 °C, corresponding to a rate of 2650 s^{-1} and a free energy of activation $\Delta G^{\ddagger}$ of 10.3 kcal/mol. In the ^1H NMR spectrum of **3**, measured in 1,2-dichloroethane at 31 °C, the two methyl resonances due to H^8 and H^7, H^9 have coalesced, which suggests that the reversible C–H bond-breaking process (Scheme VI) also occurs more readily in **3** than in **2**. Unfortunately, attempts to study this behavior at higher temperatures in $C_2H_4Cl_2$ or CH_3NO_2 were frustated by partial decomposition of the complex.

The fluxionality of complex **3** is also evident from the variation of the $^{31}P\{^1H\}$ NMR spectrum with temperature (Figure 7). At −90 °C, in addition to the usual septet due to PF_6^-, there are three resonances of equal intensity, corresponding to the inequivalent PMe_2Ph ligands, at δ 32.2 (dd, J_{PP} = 48.5, 32.6 Hz), 20.7 (d, J_{PP} = 48.5 Hz), and −8.25 (d, J_{PP} = 32.5 Hz). As the temperature is increased, the first two resonances broaden, collapse, and coalesce at −30 °C, while the remaining resonance becomes a triplet (J_{PP} = 14.8 H, calculated 16.3 Hz). The time-averaged symmetry plane generated by the $\eta^3 \rightleftarrows \eta^1$ benzyl interconversion causes a pair of PMe_2Ph ligands to become equivalent, and the value for $\Delta G^{\ddagger}$ of 10.8 kcal/mol at −30 °C obtained from the $^{31}P\{^1H\}$ NMR spectrum agrees reasonably with that estimated from the ^1H NMR spectrum. At 0 °C the spectrum consists of two somewhat broadened singlets ($w_{1/2}$ ca. 80 Hz) in a 2:1 intensity ratio at δ 25.5 and −8.6, and at 20 °C both singlets are broadened further. This behavior is probably caused by the onset of reversible C–H bond breaking, possibly accompanied by a tritopal rearrangement of the PMe_2Ph ligands, which would finally render all three equivalent.

Treatment of the unsubstituted *o*-xylylene complex $Ru\{o\text{-}(CH_2)_2C_6H_4\}(PMe_2Ph)_3$ in ether with 60% aqueous HPF_6 gives immediately the monoprotonated, agostic η^3-benzyl salt **4**. The ^1H NMR spectrum in CD_2Cl_2 at −90 °C shows a typical broad singlet at δ −2.38 due to $H^{1,2,3}$ and a pair of doublets at δ 0.75 and 2.48 (J_{HH} = 5 Hz) due to H^4 and H^5, respectively. At −30 °C the doublets broaden and at 20 °C almost collapse into the base line, as expected for the onset of a $\eta^3 \rightleftarrows \eta^1$ interconversion of the benzyl group. In the same temperature range, the peak due to $H^{1,2,3}$ sharpens owing to the increasing rate of reversible Ru–H bond cleavage. It does not shift or undergo further collapse, in contrast to the behavior of the corresponding peaks in the spectra of **2** and **3**, because there is now no methyl group with which it can average as a consequence of the $\eta^3 \rightleftarrows \eta^1$ interconversion.

Addition of an excess of HPF_6 or CF_3SO_3H to the *exo*-(*o*-xylylene)ruthenium(0) complexes or to their monoprotonation products gives salts of the dications $[Ru(\eta^6\text{-}1,2\text{-dimethylarene})L_3]^{2+}$. Diprotonation occurs with particular ease in the case of L = $P(OMe)_3$: we could only obtain the monoprotonated salt $[Ru\{\eta^3\text{-}(HCH_2)(CH_2)C_6Me_4\}\{P(OMe)_3\}_3]BF_4$ in admixture with the diprotonated salt $[Ru(\eta^6\text{-}C_6Me_6)\{P(OMe)_3\}_3](BF_4)_2$ by careful addition of $HBF_4{\cdot}OEt_2$ to $[Ru\{\eta^4\text{-}(CH_2)_2C_6Me_4\}\{P(OMe)_3\}_3]$. Unusually, the cation $[Ru(\eta^6\text{-}C_6Me_6)(PMe_2Ph)_3]^{2+}$ loses its coordinated arene in solution much more readily than do its benzene and *o*-xylene analogues. This is the reverse of the normal stability order and perhaps is a consequence of crowding in the coordination sphere. These compounds will be discussed in more detail elsewhere.

Crystal and Molecular Structures of $[Ru\{\eta^3\text{-}(HCH_2)(CH_2)C_6Me_4\}\{(Z)\text{-}Ph_2PCH{=}CHPPh_2\}(PMe_2Ph)]PF_6$ (2) and $[Ru\{\eta^3\text{-}(HCH_2)(CH_2)C_6Me_4\}(PMe_2Ph)_3]PF_6$ (3). The molecular structures of the cations in **2** and **3** are shown in Figures 8 and 9; selected bond distances and interbond angles are in Table V. The cation in **2** contains a protonated 1,2,3,4-tetramethyl-5,6-dimethylene-1,3-cyclohexadiene coordinated to a $Ru\{(Z)\text{-}Ph_2PCH{=}CHPPh_2\}(PMe_2Ph)$ fragment via a η^3-benzyl interaction from C(22), C(2), and C(1) and a three-center, two-electron (agostic) bond to C(11) and H(11A) of the *o*-methyl group in the cyclic ligand. The manner of attachment is similar to that observed in the agostic η^3-enyl complexes $[Ru(\eta^3\text{-}C_4H_7)(PMe_2Ph)_3]^+$ (**5**),[36,37]

(36) Ashworth, T. V.; Liles, D. C.; Singleton, E. *Organometallics* **1984**, *3*, 1851.

(37) Ashworth, T. V.; Singleton, E.; Laing, M.; Pope, L. *J. Chem. Soc., Dalton Trans.* **1978**, 1032.

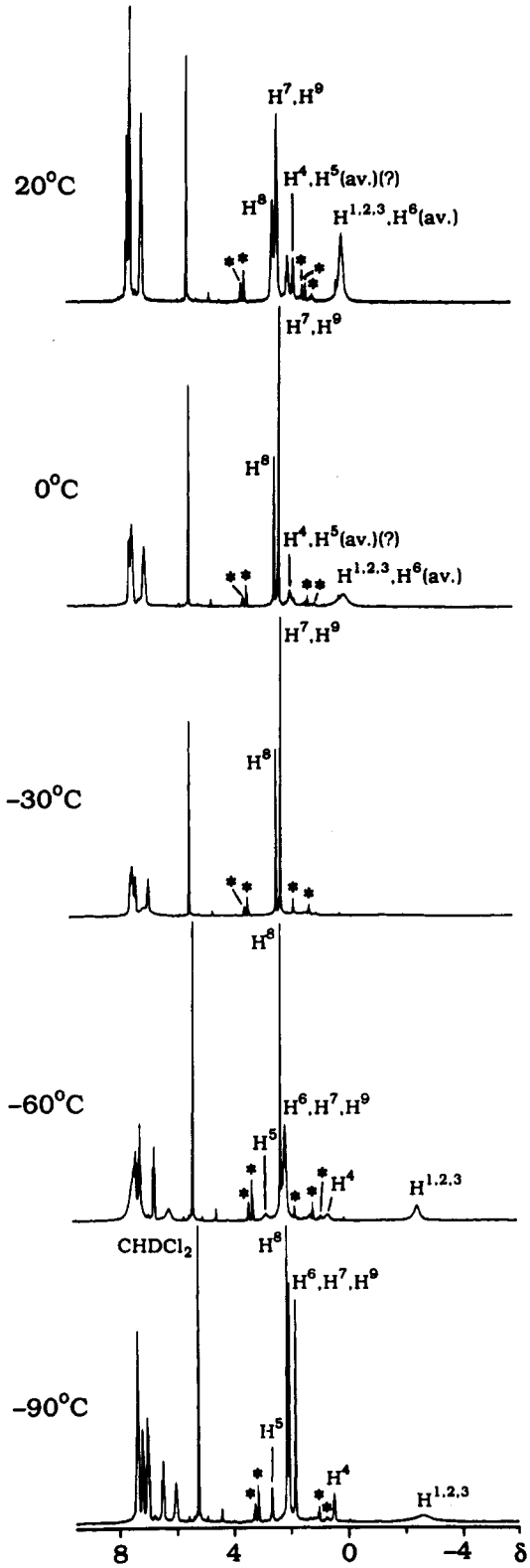

Figure 6. Variable-temperature 270-MHz ^1H NMR spectra of $[Ru\{\eta^3\text{-}(HCH_2)(CH_2)C_6Me_4\}\{P(CD_3)_2Ph\}_3]PF_6$ (**3a**) in CD_2Cl_2. Peaks marked with an asterisk are due to impurities.

$[Ru(\eta^3\text{-}C_8H_{13})\{P(OMe)Ph_2\}_3]^+$ (**6**),[38] $[Fe(\eta^3\text{-}C_8H_{13})\{P(OMe)_3\}_3]^+$ (**7**),[39] $[Mn(\eta^3\text{-}C_7H_{11})(CO)_3]^+$ (**8**),[40,41] $[Ru(\eta^3\text{-}C_{18}H_{15})(\eta^6\text{-}C_6H_3Me_3)]^+$ (**9**),[42] and $[Ru(\eta^3\text{-}C_6H_{11})(\eta^5\text{-}C_5Me_5)]^+$ (**10**).[43] The η^3-benzyl group spans two of the three available coordination sites (of six), and the agostic hydrogen atom occupies the third (here trans to P(3)). The H–Ru–P(3) moiety is substantially linear (angle 172 (1)°),

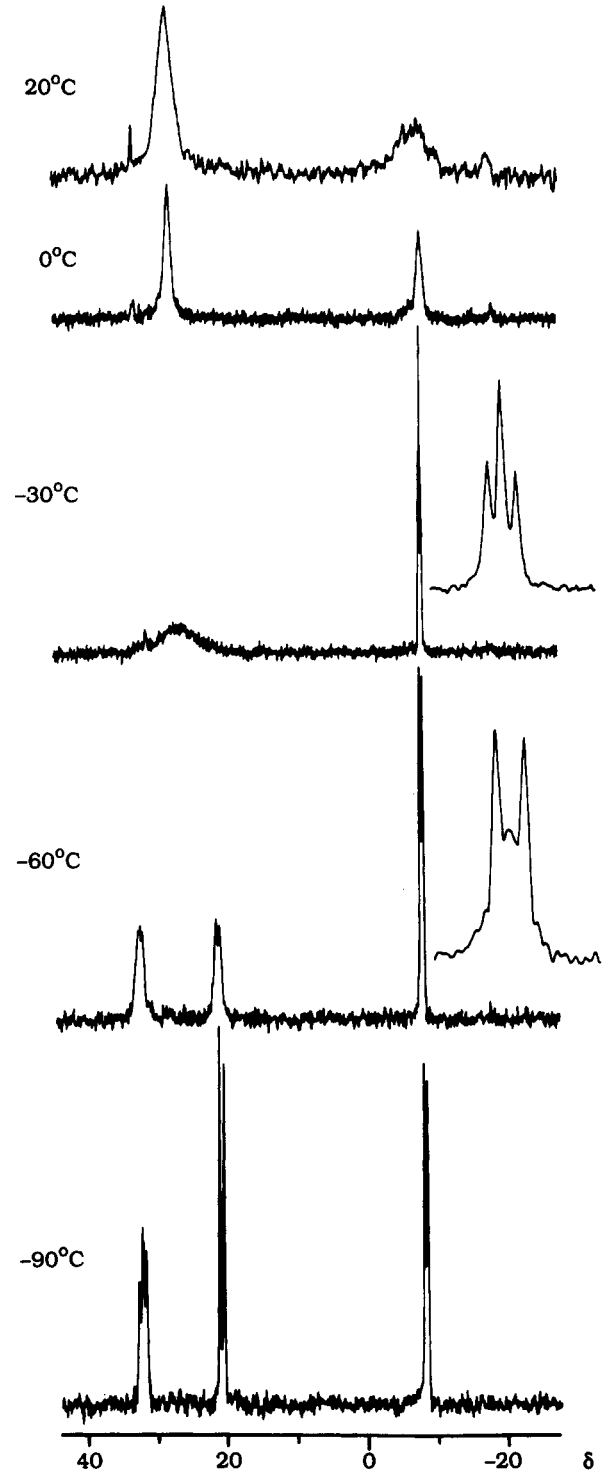

Figure 7. Variable-temperature $^{31}P\{^1H\}$ NMR spectra at 81.0 MHz of $[Ru\{\eta^3\text{-}(HCH_2)(CH_2)C_6Me_4\}\{P(CD_3)_2Ph\}_3]PF_6$ (**3a**) in CD_2Cl_2. Insets represent 17.5-fold expansions of the peak at δ −8.25. The septet due to PF_6^- is not shown.

(38) Ashworth, T. V.; Chalmers, A. A.; Meintjies, E.; Oosthuizen, H.; Singleton, E. *J. Organomet. Chem.* **1985**, *286*, 237.
(39) Brown, R. K.; Williams, J. M.; Schultz, A. J.; Stucky, G. D.; Ittel, S. D.; Harlow, R. L. *J. Am. Chem. Soc.* **1980**, *102*, 981.
(40) Brookhart, M.; Lamanna, W.; Humphrey, M. B. *J. Am. Chem. Soc.* **1982**, *104*, 2117.
(41) Schultz, A. J.; Teller, R. G.; Beno, M. A.; Brookhart, M.; Lamanna, W.; Humphrey, M. B. *Science (Washington, D.C.)* **1983**, *220*, 197.
(42) Bennett, M. A.; Pelling, S.; Robertson, G. B.; Wickramasinghe, W. A. *Organometallics* **1991**, *10*, 2166.
(43) Salzer, A.; Buchmann, B.; Schmalle, H. *Acta Crystallogr., Sect. C* **1991**, *47*, 275.

Table V. Selected Bond Lengths (Å) and Interbond Angles (deg) in $[Ru(C_{12}H_{17})(Ph_2PCH{=}CHPPh_2)(PMe_2Ph)]PF_6$ (2) and $[Ru(C_{12}H_{17})(PMe_2Ph)_3]PF_6$ (3)

	2	3		2	3
Ru-P(1)	2.303 (1)	2.270 (1)	C(4)-C(44)	1.518 (11)	1.559 (10)
Ru-P(2)	2.329 (1)	2.286 (2)	C(4)-C(5)	1.416 (8)	1.386 (10)
Ru-P(3)	2.262 (1)	2.341 (2)	C(5)-C(55)	1.536 (11)	1.530 (11)
Ru-C(1)	2.358 (4)	2.408 (7)	C(5)-C(6)	1.374 (7)	1.385 (9)
Ru-C(2)	2.342 (4)	2.364 (7)	C(6)-C(66)	1.504 (8)	1.495 (9)
Ru-C(11)	2.416 (5)	2.333 (9)	C(6)-C(1)	1.409 (6)	1.417 (8)
Ru-C(22)	2.164 (5)	2.283 (10)	C(11)-H(11A)	1.01 (5)	
Ru-H(11A)	1.92 (4)		C(11)-H(11B)	0.95 (5)	
P(1)-C(111)	1.828 (5)	1.826 (9)			
P(1)-C(121)	1.811 (6)	1.841 (7)	C(22)-H(11C)	1.04 (5)	
P(1)-C(131)	1.823 (6)	1.863 (11)	C(22)-H(22A)	0.92 (5)	
			C(22)-H(22B)	0.92 (5)	
P(2)-C(201)	1.810 (4)		C(201)-C(301)	1.305 (6)	
P(2)-C(211)	1.819 (4)	1.822 (6)	C(201)-H(201)	0.88 (4)	
P(2)-C(221)	1.846 (3)	1.834 (6)	C(301)-H(301)	0.87 (4)	
P(2)-C(231)		1.861 (9)	H-C (Ph)	0.95[a]	0.95[a]
P(3)-C(301)	1.819 (4)		H-C (Me)	0.74 (7)-1.21 (8)	
P(3)-C(311)	1.825 (4)	1.821 (6)	F(1)-P(4)	1.517 (6)	1.593 (9)
P(3)-C(321)	1.834 (4)	1.874 (11)	F(2)-P(4)	1.495 (6)	1.437 (7)
P(3)-C(331)		1.805 (6)	F(3)-P(4)	1.552 (6)	1.493 (9)
C(1)-C(11)	1.496 (7)	1.472 (8)	F(4)-P(4)	1.555 (7)	1.433 (7)
C(1)-C(2)	1.433 (6)	1.389 (6)	F(5)-P(4)	1.512 (5)	
C(2)-C(22)	1.453 (7)	1.483 (9)	F(6)-P(4)	1.537 (5)	
C(2)-C(3)	1.430 (6)	1.427 (8)	F(5)-P(5)		1.581 (6)
C(3)-C(33)	1.511 (8)	1.486 (9)	F(6)-P(5)		1.527 (7)
C(3)-C(4)	1.382 (7)	1.366 (9)	F(7)-P(5)		1.474 (9)
P(1)-Ru-P(2)	97.88 (4)	95.45 (6)	C(5)-C(4)-C(44)	119.3 (5)	119.1 (6)
P(1)-Ru-P(3)	91.97 (4)	97.77 (6)	C(55)-C(5)-C(4)	119.1 (6)	120.5 (6)
P(1)-Ru-C(1)	136.6 (1)	128.2 (2)	C(6)-C(5)-C(4)	121.3 (5)	120.5 (6)
P(1)-Ru-C(22)	91.3 (1)	98.2 (2)	C(6)-C(5)-C(55)	119.6 (6)	119.0 (6)
P(1)-Ru-H(11A)	83 (1)		C(66)-C(6)-C(1)	119.7 (5)	119.6 (6)
P(2)-Ru-P(3)	83.70 (3)	92.9 (7)	C(5)-C(6)-C(1)	119.2 (4)	119.3 (5)
P(2)-Ru-C(1)	103.7 (1)	102.0 (1)	C(5)-C(6)-C(66)	121.1 (5)	121.1 (6)
P(2)-Ru-C(22)	169.3 (1)	163.6 (2)	C(1)-C(11)-H(11A)	118 (2)	
P(2)-Ru-H(11A)	90 (1)		C(1)-C(11)-H(11B)	112 (3)	
P(3)-Ru-C(1)	127.2 (1)	129.0 (1)	C(1)-C(11)-H(11C)	120 (2)	
P(3)-Ru-C(22)	101.7 (1)	94.4 (2)	H(11A)-C(11)-H(11B)	98 (4)	
P(3)-Ru-H(11A)	172 (1)		H(11A)-C(11)-H(11C)	96 (3)	
Ru-P(2)-C(201)	107.9 (1)		H(11B)-C(11)-H(11C)	110 (4)	
Ru-P(3)-C(301)	109.0 (1)		C(2)-C(22)-H(22A)	120 (3)	
C(11)-C(1)-C(2)	116.4 (4)	117.1 (4)	C(2)-C(22)-H(22B)	120 (3)	
C(6)-C(1)-C(2)	120.0 (4)	119.3 (5)	H(22A)-C(22)-H(22B)	107 (4)	
C(6)-C(1)-C(11)	122.7 (4)	123.4 (5)	C-C-H (Me)[a]	99 (6)-121 (4)	
C(22)-C(2)-C(1)	116.1 (4)	115.1 (5)	H-C-H (Me)[a]	80 (7)-143 (9)	
C(3)-C(2)-C(1)	119.5 (4)	120.6 (5)	P(2)-C(201)-C(301)	118.4 (3)	
C(3)-C(2)-C(22)	124.3 (4)	124.1 (5)	P(2)-C(201)-H(201)	119 (2)	
C(33)-C(3)-C(2)	118.7 (5)	120.6 (6)	C(301)-C(201)-H(201)	122 (2)	
C(4)-C(3)-C(2)	118.2 (4)	118.4 (5)	P(3)-C(301)-C(201)	119.5 (3)	
C(4)-C(3)-C(33)	123.0 (5)	121.1 (6)	P(3)-C(301)-H(301)	117 (3)	
C(44)-C(4)-C(3)	119.2 (6)	119.1 (7)	C(201)-C(301)-H(301)	124 (3)	
C(5)-C(4)-C(3)	121.5 (5)	121.8 (6)			

[a] Excludes methyl group $C(22)H_3$.

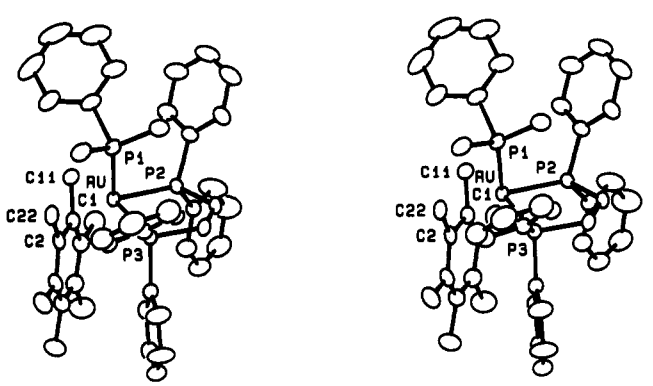

Figure 8. Molecular structure of the cation of $[Ru\{\eta^3\text{-}(HCH_2)(CH_2)C_6Me_4\}\{(Z)\text{-}Ph_2PCH{=}CHPPh_2\}(PMe_2Ph)]PF_6$ (2) with 30% ellipsoids. Hydrogen atoms are omitted for clarity.

a feature which is also observed for the trans-disposed H-M-L fragments in complexes 6-8.[44] The Ru-H distance (1.92 (4) Å) is in good agreement with M-H distances determined by X-ray crystallography for complexes 6-10 (range 1.80 (7)-2.08 (7) Å), but the pattern of M-C distances differs. Thus, whereas in 6-10 the shortest M-C distances are those to the two central carbon atoms of the η^3-butenyl moiety, in 2 the Ru-C distances increase progressively from the exocyclic terminus of the η^3-benzyl group (Ru-C(22) = 2.164 (5) Å, Ru-C(2) = 2.342 (4) Å, Ru-C(1) = 2.358 (4) Å, Ru-C(11) = 2.416 (5) Å). This pattern of distances to the first three carbon atoms is, however, typical of mononuclear η^3-benzyl complexes of the middle and late d-block elements; cf. the corresponding bond lengths in the following compounds (all distances in Å): $Mo(\eta^5\text{-}C_5H_5)(\eta^3\text{-}CH_2C_6H_4Me\text{-}p)(CO)_2$ (2.269 (7), 2.364 (5), and 2.480 (6)),[45] $Pd(acac)(\eta^3\text{-}CPh_2C_6H_4)$ (2.103, 2.159, and 2.202 (average values)),[46] $[Pt\{t\text{-}Bu_2P(CH_2)_3PBu_2\text{-}$

(44) The agostic hydrogen atom in complex 5 was not located.
(45) Cotton, F. A.; La Prade, M. D. J. Am. Chem. Soc. 1968, 90, 5418.

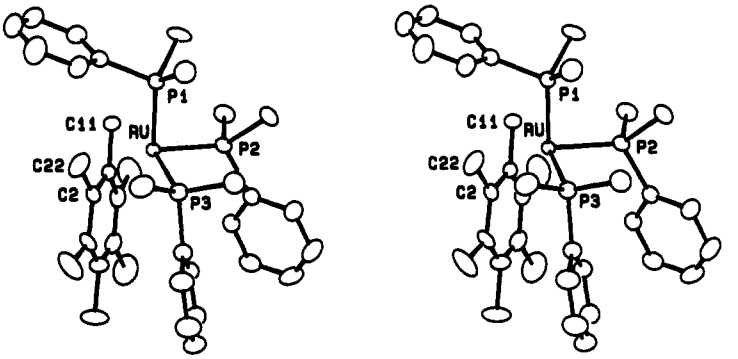

Figure 9. Molecular structure of the cation in $[Ru\{\eta^3\text{-}(HCH_2)(CH_2)C_6Me_4\}(PMe_2Ph)_3]PF_6$ (3) with 30% ellipsoids.

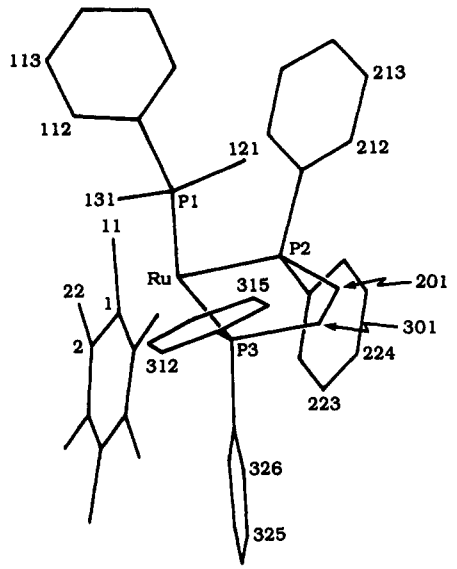

Figure 10. Atom nomenclature for the cation of $[Ru\{\eta^3\text{-}(HCH_2)(CH_2)(C_6Me_4)\}\{(Z)\text{-}Ph_2PCH{=}CHPPh_2\}(PMe_2Ph)]PF_6$ (2).

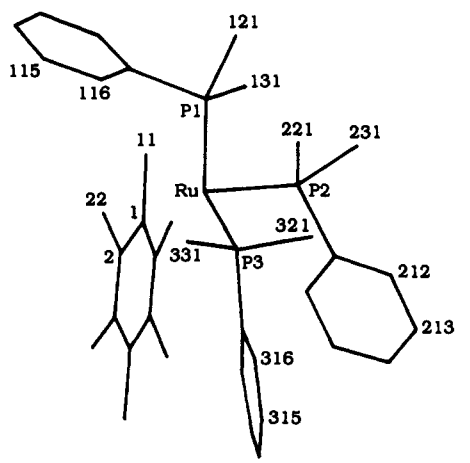

Figure 11. Atom nomenclature for the cation of $[Ru\{\eta^3\text{-}(HCH_2)(CH_2)C_6Me_4\}(PMe_2Ph)_3]PF_6$ (3).

$t\}(\eta^3\text{-}anti\text{-}1\text{-}MeCHC_6H_4Br\text{-}4)]BF_4$ (2.163 (11), 2.242 (10), and 2.446),[47] $NiCl(\eta^3\text{-}CH_2C_6H_4Me\text{-}o)(PMe_3)$ (1.930 (8), 2.050 (8), and 2.318 (9)),[48] $Co(\eta^3\text{-}CH_2C_6H_4)\{P(OMe)_3\}_3$ (2.036 (3), 2.117 (3), and 2.408 (3)),[49] $Rh(\eta^3\text{-}CH_2C_6Me_5)\{P(O\text{-}i\text{-}Pr)_3\}_2$ (2.128 (3), 2.246 (3), and 2.453 (3)),[50] $Rh(\eta^3\text{-}CH_2C_6H_4Me\text{-}o)(PPh_3)_2$ (2.140 (8), 2.212 (6), and 2.286 (5)),[51] and $Rh(\eta^3\text{-}anti\text{-}1\text{-}MeC_6H_4Me\text{-}o)$(1,5-COD) (2.138 (5), 2.188 (5), and 2.292 (4)).[52]

In **3**, unlike **2**, the distances from the ruthenium to the terminal carbon atoms of the butenyl moiety are almost equal to within experimental error (Ru–C(11) = 2.333 (9) Å, Ru–C(22) = 2.283 (10) Å), consistent with **3** representing not only a symmetrized average over pairs of crystallographically independent cations (see above) but also a chemical average in which both C(11) and C(22) are protonated alternately. Formulation of **3** as a diene–hydride rather than an agostic enyl species would appear to be precluded firmly (a) by the overall stereochemical similarity to **2** and (b) by the fact that inclusion of a hydride ligand in the only apparently vacant space (trans to P(1)) generates unacceptably short H···C nonbonding separations of ca. 1.7 Å.

Since the coordinates of the agostic hydrogen atom in **2** are well-defined by the X-ray experiment, the formalism devised by Crabtree et al.[53] can be used to provide a measure of the strength of interaction. For **2**, the Ru–H(agostic) distance is 1.92 (4) Å, the C–H distance is 1.01 (5) Å, and the C–H–Ru angle is 107 (3)°. The corresponding values of d_{bp} (the distance from the metal atom to the C–H bond-pair electron centroid) and of $r_{bp} = d_{bp} - r_m$, where r_m is the metal atom covalent radius, are respectively 1.99 and 0.72 Å. The r_{bp} value is similar to that in the iron(0) complex **7** (0.79 Å)[39] and intermediate between those in $[Ru(\eta^3\text{-}C_8H_{13})\{P(OMe)Ph_2\}_3]^+$ (**6**; 0.89 Å)[38] and $[Ru(\eta^3\text{-}C_{18}H_{15})(\eta^6\text{-}C_6H_3Me_3)]^+$ (**9**; 0.62 Å).[42] Because r_{bp} values in the series of ruthenium compounds vary approximately as the Ru···C distance in the agostic bond, the interaction in $[Ru(\eta^3\text{-}C_4H_7)(PMe_2Ph)_3]^+$ (**5**),[36,37] for which no hydrogen atoms were located directly, must also be accounted as strong (r_{bp} ca. 0.66). The fact that the structurally similar complexes **5** and **6** give very different r_{bp} values suggests that variations in the strength of the agostic interaction are probably caused mainly by steric rather than electronic effects, at least in this series of ruthenium complexes.

The Ru–P bond lengths (2.262 (1)–2.329 (1) Å in **2**; 2.270 (1)–2.341 (2) Å in **3**) are in the same range as those for **5** (2.28 (1)–2.34 (1) Å)[37] and **6** (2.223 (2)–2.350 (2) Å).[38] In **2**, **3**, and **6**, the distances to the two phosphorus atoms trans to the butenyl fragments differ significantly (2.262 (1), 2.329 (1) Å in **2**; 2.286 (2), 2.341 (2) Å in **3**; 2.223 (2),

(46) Sonoda, A.; Bailey, P. M.; Maitlis, P. M. *J. Chem. Soc., Dalton Trans.* **1979**, 346.
(47) Crascall, L. E.; Litster, J. A.; Redhouse, A. D.; Spencer, J. L. *J. Organomet. Chem.* **1990**, *394*, C35.
(48) Carmona, E.; Marin, J. M.; Paneque, M.; Poveda, M. L. *Organometallics* **1987**, *6*, 1757.
(49) Bleeke, J. R.; Burch, R. R.; Coulman, C. L.; Schardt, B. C. *Inorg. Chem.* **1981**, *20*, 1316.
(50) Burch, R. R.; Muetterties, E. L.; Day, V. W. *Organometallics* **1982**, *1*, 188.
(51) Chappell, S. D.; Cole-Hamilton, D. J.; Galas, A. M. R.; Hursthouse, M. B.; Walker, N. P. C. *Polyhedron* **1985**, *4*, 121.
(52) Stühler, H.-O.; Pickardt, J. *Z. Naturforsch., B* **1981**, *36*, 315.
(53) Crabtree, R. H.; Holt, E. M.; Lavin, M.; Morehouse, S. M. *Inorg. Chem.* **1985**, *24*, 1986.

2.350 (2) Å in **6**), probably owing to asymmetry in the nonbonding intramolecular interactions and the unsymmetrical coordination of the η^3-enyl ligands. As is true also for **5**,[36,37] **6**,[38] and **7**,[39] the shortest M–P distance in each instance is that which is approximately trans to the agostic hydrogen. Differences in the lengths of the Ru–P bonds cis to the butenyl ligands (2.303 (1) Å, **2**; 2.270 (1) Å, **3**; 2.302 (2) Å, **6**) and the greater than 90° values for the unconstrained P–Ru–P angles (92.0–97.9°, **2**; 92.9–97.8°, **3**; 91.2–98.4°, **6**) can also be attributed to asymmetric nonbonding interactions. The constrained P–Ru–P angle in **2** (the internal angle of the chelate M–P ring) is less than 90° (83.70 (3)°), and other internal angles deviate by at most 1.6° from their ideal values, indicating that the five-membered ring is relatively unstrained.

The lattices of **2** and **3** consist of discrete cations and anions separated by normal van der Waals contact distances. The shortest interion contacts involving hydrogen atoms are F(6)···H(11C) (2.63 Å) in **2** and F(6)···H(215) (2.48 Å) in **3** (for which phenyl hydrogen atoms only were included in the scattering model); the shortest interion contacts not involving hydrogen atoms are F(4)···C(121) (3.16 Å) in **2** and F(5)···C(55) (3.11 Å) in **3**. Like the cations, the PF_6 anions in **2** occupy general sites in the lattice and exhibit no crystallographically imposed symmetry. In **3**, the PF_6 anions are constrained, under $C2/c$ symmetry, to occupy two sets of special sites, one having C_i and the other C_2 symmetry. In all instances the fluorine atoms have very anisotropic thermal parameters, the maximum/minimum rms amplitudes for **2** and **3** being 0.65/0.23 and 0.87/0.19 Å, respectively. The P–F distances (average 1.53 Å, **2**; 1.51 Å, **3**) are, therefore, much less than the expected value of ca. 1.60 Å. Thermal parameters for PF_6 derived from the 130 K data for **3** average about 40% less than those at room temperature and are consistent with a dynamic rather than static smearing process. Carbon atom amplitudes in **2** and **3** are considerably less than those for fluorine but can still be large (e.g. $(\mu_{max}^2)^{1/2}$ is 0.46–0.49 Å for C(33)–C(55) in **3**, 0.44–0.50 Å for C(113)–C(115) in **2**, and 0.45–0.47 Å for C(225)–C(226) in **2**).

Discussion

The facile double deprotonation of (η^6-1,2-dimethylarene)ruthenium(II) cations to exo-coordinated (η^4-*o*-xylylene)ruthenium(0) complexes (eq 2) is a further example of the increase in acidity of benzylic protons as a result of η^6 coordination to metal ions[54] and provides a convenient alternative to syntheses based on the reaction of lithiated methylarenes with $RuCl_2L_4$.[10,11] Our reactions do, however, differ from the formally similar double deprotonation of $[Ru(\eta^6\text{-}C_6Me_6)_2]^{2+}$, which gives an endo-coordinated tetramethyl-*o*-xylylene (eq 1).[13] It might be supposed that the first step in our reactions is replacement of weakly bound NO_3^- or $CF_3CO_2^-$ by the external ligand L′ to generate a dicationic species (eq 3), which would be expected

$$[RuX(\eta^6\text{-}C_6Me_6)L_2]^+ + L' \rightarrow [Ru(\eta^6\text{-}C_6Me_6)L_2L']^{2+} + X^- \quad (3)$$

X = NO_3, CF_3CO_2; L′ = PMe_2Ph; L_2 = $Ph_2PCH_2CH_2PPh_2$, (*Z*)-$Ph_2PCH{=}CHPPh_2$, $2PMe_2Ph$

to be readily deprotonated. In preliminary studies, however, we have found that treatment of the *o*-xylene complex $[Ru(\eta^6\text{-}1,2\text{-}C_6H_4Me_2)(PMe_2Ph)_3]^{2+}$ with KO-*t*-Bu gives only

(54) Moulines, F.; Astruc, D. *J. Chem. Soc., Chem. Commun.* **1989**, 614 and references cited therein.

Scheme VII

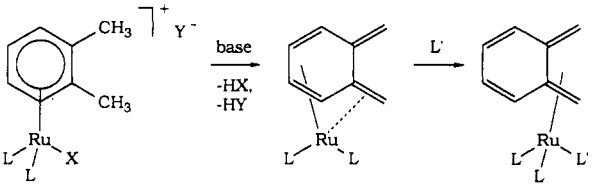

the endo-coordinated *o*-xylylene complex $Ru\{\eta^4\text{-}endo\text{-}C_6H_4(CH_2)_2\}(PMe_2Ph)_3$, without any of the corresponding exo-coordinated isomer.[55] This result is similar to that of eq 1 and suggests that deprotonation of 18e 1,2-dimethyl arene–metal dications will give successively *endo*-η^3-*o*-methylbenzyl and *endo*-*o*-xylylene complexes, unless ligand dissociation intervenes. In agreement, removal of one proton from the coordinatively unsaturated rhodium(I) cation $[Rh(\eta^6\text{-}C_6Me_6)\{P(O\text{-}i\text{-}Pr)_3\}_2]^+$ gives exclusively the *exo*-(η^3-pentamethylbenzyl)rhodium(I) complex $Rh(\eta^3\text{-}CH_2C_6Me_5)\{P(O\text{-}i\text{-}Pr)_3\}_2$, although this species may be in thermal equilibrium with an endo isomer, $Rh(\eta^5\text{-}C_6Me_5CH_2)\{P(O\text{-}i\text{-}Pr)_3\}_2$.[50]

Clearly, dications of the type $[Ru(\eta^6\text{-}1,2\text{-dimethylarene})L_2L']^{2+}$ are not intermediates in our deprotonations. We suggest instead that the cations $[RuX(\eta^6\text{-}1,2\text{-dimethylarene})L_2]^+$ are deprotonated directly to give the short-lived intermediate Ru(*o*-xylylene)L_2 (**10**) (Scheme VII). The 16e ruthenium atom in this species can relieve its electronic unsaturation by accepting a pair of electrons from one of the exo double bonds, thus providing a pathway for the ruthenium atom to move from the endo to the exo site. If this process takes place more rapidly than the intermediate is intercepted by L′, the exo-coordinated *o*-xylylene, which is probably more stable than the endo isomer, will be formed. Experiments to test these proposals are planned. An (*o*-xylylene)$Cr(CO)_3$ complex analogous to **10** is believed to be an intermediate in the intramolecular interconversion of *syn*- and *anti*-(1-ethoxy-1,2-dihydrocyclobutabenzene)$Cr(CO)_3$; it has been trapped in the form of its [4 + 2] cycloaddition product with (*E*)-$Me_3SiCH{=}CHSiMe_3$.[56]

The double deprotonation of $[RuX(\eta^6\text{-}1,2\text{-dimethylarene})L_2]^+$ in the presence of ligand L′ undoubtedly occurs stepwise via the agostic *endo*-η^3-*o*-methylbenzyl cations that we have isolated by monoprotonation of the *o*-xylylene complexes. These cations exhibit fluxional behavior characteristic of both agostic species (reversible cleavage of M–H bonds, reversible cleavage of C–H bonds) and of η^3-benzyl complexes ($\eta^3 \rightleftarrows \eta^1$ interconversion). The M–H bond cleavage evidently has a lower activation energy than the C–H bond cleavage; this is true also for the closely related agostic cations $[M(\eta^3\text{-dienyl})L_3]^+$ (M = Fe, L = CO, PR_3; M = Ru, L = PR_3, AsR_3)[37,57,58] but is in contrast to the agostic cations $[Ru(\eta^3\text{-dienyl})(\eta^6\text{-arene})]^+$,[42,59] for which the reverse order holds. The fluxionality of the η^3-benzyl group in the d^6 metal complexes **1**–**4** seems to resemble that in $M(\eta^5\text{-}C_5H_5)(\eta^3\text{-}CH_2Ar)(CO)_2$ (M = Mo, W), for which a 16e η^1-benzyl intermediate has been proposed.[32] In contrast, in d^8 metal complexes such as $[Pd(\eta^3\text{-}CH_2Ph)(PEt_3)_2]^+$,[35] $Rh(\eta^3\text{-}CH_2C_6Me_5)\{P(O\text{-}i\text{-}Pr)_3\}_2$,[50] M-

(55) Bennett, M. A.; Goh, L. Y.; Mitchell, T. R. B. Unpublished observations.

(56) Kündig, E. P.; Bernardinelli, G.; Leresche, J.; Romanens, P. *Angew. Chem., Int. Ed. Engl.* **1990**, *29*, 407.

(57) Brookhart, M.; Whitesides, T. H.; Crockett, J. M. *Inorg. Chem.* **1976**, *15*, 1550.

(58) Ittel, S. D.; Van-Catledge, F. A.; Jesson, J. P. *J. Am. Chem. Soc.* **1979**, *101*, 6905.

(59) Bennett, M. A.; McMahon, I. J.; Pelling, S.; Brookhart, M.; Lincoln, D. M. *Organometallics* **1992**, *11*, 127.

(η^3-CPh_3)(acac) (M = Pd, Pt),[60] and [Pt{t-$Bu_2P(CH_2)_3P$-t-Bu_2}(η^3-*anti*-1-MeCHAr)]$^+$ [47] the metal undergoes a [1,5]-suprafacial shift between equivalent η^3-benzyl sites which, in the first two cases, is rapid on the ^{1}H NMR time scale, even at low temperature.

Supplementary Material Available: Summary tables of crystal data and data collection and refinement details and listings of anisotropic thermal parameters for **2** and **3** and a table of hydrogen atom coordinates for **2** (9 pages). Ordering information is given on any current masthead page.

OM920009C

(60) Mann, B. E.; Keasey, A.; Sonoda, A.; Maitlis, P. M. *J. Chem. Soc., Dalton Trans.* **1979**, 338.

^{1}H NMR Detection of Cationic Organopalladium(IV) Intermediates in Oxidative-Addition Reactions and the Structure of *fac*-$PdBrMe_2(CH_2COPh)(bpy)$

Peter K. Byers,[1a,b] Allan J. Canty,*,[1a] Brian W. Skelton,[1c] Peter R. Traill,[1a] Andrew A. Watson,[1a] and Allan H. White[1c]

Chemistry Department, University of Tasmania, Hobart, Tasmania, Australia 7001, and Department of Physical and Inorganic Chemistry, University of Western Australia, Nedlands, Western Australia 6009

Received April 14, 1992

Phenacyl bromides react with dimethylpalladium(II) complexes $PdMe_2(L_2)$ (L_2 = bpy, phen) to form the palladium(IV) complexes *fac*-$PdBrMe_2(CH_2COAr)(L_2)$ (Ar = Ph, *p*-C_6H_4Br), which have both methyl groups trans to the bidentate nitrogen donor ligand. ^{1}H NMR studies of the oxidative addition of phenacyl bromides to $PdMe_2$(bpy) in $(CD_3)_2CO$ at −5 °C indicate the formation of two similar cationic intermediates, prior to formation of the neutral product. As the cations have only one of the methyl groups trans to bpy, configurational changes at palladium occur on cation formation and on conversion of the cations to the neutral product. It is proposed that one of the cations may be stabilized via an intramolecularly coordinated phenacyl group, $[PdMe_2(CH_2COAr\text{-}C,O)(L_2)]^+$. A single cation, exhibiting NMR spectra similar to those of the cations of the bpy complexes, is detected as an intermediate in the reaction of $PdMe_2$(phen) with $ArCOCH_2Br$. A cation has also been detected for the reaction of $PdMe_2$(bpy) with CD_3I in $(CD_3)_2CO$ at −50 °C, prior to formation of $PdIMe_2(CD_3)$(bpy). Both the cation, most likely $[PdMe_2(CD_3)(bpy)((CD_3)_2CO)]^+$, and the neutral product display scrambled Me and CD_3 groups, in contrast to the trans oxidative addition reported for the analogous reaction of $PtMe_2$(bpy) with CD_3I. Crystals of $PdBrMe_2(CH_2COAr)$(bpy) are orthorhombic, space group *Pbca*, with a = 19.554 (3) Å, b = 15.007 (9) Å, c = 13.282 (4) Å, and Z = 8.

Introduction

The classic S_N2 mechanism for oxidative addition of alkyl halides to d^8 metal centers is expected to require the formation of a cation intermediate (eq 1).[2,3] However, spectroscopic detection of intermediate cations appears to be restricted to two platinum(II,IV) systems,[4,5] presumably because reaction ii is very fast under the conditions usually required for monitoring reaction i.

$$\underset{d^8}{M} + RX \xrightarrow{(i)} \underset{d^6}{MR^+X^-} \xrightarrow{(ii)} \underset{d^6}{MXR} \qquad (1)$$

The recent emergence of an organometallic chemistry of palladium(IV),[6-9] involving the reaction of alkyl halides with palladium(II) d^8 complexes, is providing new systems for the examination of mechanisms in oxidative-addition chemistry. Kinetic studies indicate occurrence of the S_N2 mechanism for the reaction of $PdMe_2(L_2)$ (L_2 = 2,2′-bipyridyl (bpy), 1,10-phenanthroline (phen)) with iodomethane and benzyl bromide.[10] Consistent with this mechanism, the tetramethylethylenediamine complex $PdMe_2$(tmeda) reacts with methyl triflate in CD_3CN to form $[PdMe_3(tmeda)(NCCD_3)]^+SO_3CF_3^-$.[8a] We report here further developments in the synthetic chemistry of palladium(IV), resulting in ^{1}H NMR detection of cation intermediates in oxidative-addition reactions. The studies reveal facile isomerization processes during oxidative addition of phenacyl bromides to $PdMe_2(L_2)$, and a reexamination of the reaction of iodomethane with $PdMe_2$(bpy) at −50 °C has also revealed the occurrence of a cation intermediate. A preliminary report of part of this work has appeared.[11]

Results and Discussion

Synthesis and Characterization of Palladium(IV) Complexes $PdBrMe_2(CH_2COAr)(L_2)$ (L_2 = bpy, phen; Ar = Ph, *p*-C_6H_4Br). The complexes formed on reaction of $PdMe_2(L_2)$ with the organo bromides at 0 °C and were isolated by workup at this temperature. ^{1}H NMR spectra for $CDCl_3$ solutions are readily interpretable, with singlets for PdMe and CH_2 groups, and equivalence of pyridyl rings

(1) (a) University of Tasmania. (b) Present address: School of Chemistry, The University of Birmingham, Birmingham B15 2TT, England. (c) University of Western Australia.
(2) Chock, P. B.; Halpern, J. *J. Am. Chem. Soc.* **1966**, *88*, 3511.
(3) Collman, J. P.; Hegedus, L. S.; Norton, J. R.; Finke, R. G. *Principles and Applications of Organotransition Metal Chemistry*; University Science Books: Mill Valley, CA, 1987; Chapter 5.
(4) Puddephatt, R. J.; Scott, J. D. *Organometallics* **1985**, *4*, 1221.
(5) Crespo, M.; Puddephatt, R. J. *Organometallics* **1987**, *6*, 2548.
(6) Byers, P. K.; Canty, A. J.; Skelton, B. W.; White, A. H. *J. Chem. Soc., Chem. Commun.* **1986**, 1722.
(7) Canty, A. J. *Acc. Chem. Res.* **1992**, *25*, 83.
(8) (a) de Graaf, W.; Boersma, J.; Smeets, W. J. J.; Spek, A. L.; van Koten, G. *Organometallics* **1989**, *8*, 2907. (b) de Graaf, W.; Boersma, J.; van Koten, G. *Organometallics* **1990**, *9*, 1479.
(9) Catellani, M.; Chiusoli, G. P. *J. Organomet. Chem.* **1988**, *346*, C27. Catellani, M.; Mann, B. E. *J. Organomet. Chem.* **1990**, *390*, 251.
(10) (a) Byers, P. K.; Canty, A. J.; Crespo, M.; Puddephatt, R. J.; Scott, J. D. *Organometallics* **1988**, *7*, 1363. (b) Aye, K.-T.; Canty, A. J.; Crespo, M.; Puddephatt, R. J.; Scott, J. D.; Watson, A. A. *Organometallics* **1989**, *8*, 1518.
(11) Canty, A. J.; Watson, A. A.; Skelton, B. W.; White, A. H. *J. Organomet. Chem.* **1989**, *367*, C25.

0276-7333/92/2311-3085$03.00/0